

Efficient Computing of Nonlinear Higher-Order Fractional Integro-Differential Equations via Aboodh-ADM Technique

Salma Trabelsi^{1,#} and Maha M. Hamood^{2,3,*,#}

¹ Department of Mathematics and Statistics, College of Science, King Faisal University, Hofuf, Al Ahsa, 31982, Saudi Arabia

² Department of Mathematics, Taiz University, Taiz, 6803, Yemen

³ Department of Mathematics, Dr. Babasaheb Ambedkar Marathwada University, Chh. Sambhajinagar, 431004, India

These authors contributed equally to this work

INFORMATION

Keywords:

Integro-fractional Volterra
Fredholm-higher-order
Adomian decomposition method
Aboodh transform

DOI: 10.23967/j.rimni.2025.10.67393

Revista Internacional
Métodos numéricos
para cálculo y diseño en ingeniería

RIMNI



UNIVERSITAT POLITÈCNICA
DE CATALUNYA
BARCELONATECH

In cooperation with
CIMNE[®]

Efficient Computing of Nonlinear Higher-Order Fractional Integro-Differential Equations via Aboodh-ADM Technique

Salma Trabelsi^{1, #} and Maha M. Hamood^{2, 3, *, #}

¹Department of Mathematics and Statistics, College of Science, King Faisal University, Hofuf, Al Ahsa, 31982, Saudi Arabia

²Department of Mathematics, Taiz University, Taiz, 6803, Yemen

³Department of Mathematics, Dr. Babasaheb Ambedkar Marathwada University, Chh. Sambhajinagar, 431004, India

[#]These authors contributed equally to this work

ABSTRACT

This paper introduces a novel semi-analytical method for solving nonlinear higher-order fractional Volterra-Fredholm integro-differential equations (FIDEs) of Hammerstein type. By combining the Aboodh transform with the Adomian Decomposition Method (ADM), the proposed approach efficiently handles Caputo fractional derivatives and nonlocal integral operators. The solution is derived as a rapidly convergent infinite series via the inverse Aboodh transform, offering analytical insight even in the absence of closed-form solutions. Rigorous stability analysis and convergence criteria are established, demonstrating the method's numerical stability and confirming an algebraic order of convergence dependent on fractional order and discretization parameters. Truncated series solutions yield high-accuracy approximations, validated through numerical examples that highlight the method's reliability, computational efficiency, and robustness for memory-dependent dynamics. The framework is broadly applicable to engineering and applied mathematics problems requiring precise modeling of nonlocal phenomena.

OPEN ACCESS

Received: 02/05/2025

Accepted: 25/06/2025

Published: 15/08/2025

DOI

10.23967/j.rimni.2025.10.67393

Keywords:

Integro-fractional Volterra
Fredholm-higher-order
Adomian decomposition method
Aboodh transform

Nomenclature

Symbol	Meaning
\mathfrak{w}	Order of LHS fractional derivative
q	Order of first fractional derivative
q^*	Order of second fractional derivative
ω_0	Weight of first integral term
ω_0^*	Weight of second integral term
$\kappa(\tau)$	Forcing function
$h(\tau)$	Exact solution

1 Introduction

The mathematical foundations for fractional differential equations have been well-established in the literature, with comprehensive treatments of both theory and applications [1,2]. These works provide essential frameworks for understanding and solving fractional-order problems through analytical methods [3]. For classical integral equations, both linear and nonlinear cases have been thoroughly investigated, offering fundamental solution methods and practical applications [4]. Together, these references form a complete theoretical basis spanning both fractional and classical approaches to differential and integral equations.

The study of integral and integro-differential equations has evolved through various analytical and numerical approaches. Early theoretical foundations were established in classical texts on integral equations [5,6], which provided fundamental solution methods and applications. The modified Aboodh-Adomian approach [7] further improved solutions for integro-differential equations. For fractional integro-differential equations, study [8] demonstrated the effectiveness of the Adomian Decomposition Method (ADM), building upon these classical foundations. Recent advances have combined ADM with transform methods, particularly the Aboodh transform, as shown in works like [9] for heat transfer problems and [10] for biological systems modeling, while study [11] extended ADM applications to partial differential equations. This progression from classical theory to modern hybrid methods demonstrates the ongoing development of effective analytical tools for increasingly complex equations.

Recent advances in solving fractional differential equations (FDEs) include both analytical and discretization-based techniques. Semi-analytical methods like the Homotopy Perturbation Method (HPM) [12] and Variational Iteration Method (VIM) [13] decompose nonlinearities via perturbation or correction functionals.

Spline-based approximation methods have emerged as powerful tools, including:

- Hyperbolic non-polynomial spline method [14], first developed by [15] for ordinary differential equations and later extended to FDEs by [16]
- Rational non-polynomial spline method [17], with foundational work by [18] and fractional applications in [19]
- Logarithmic non-polynomial spline method [20], introduced by [21] for singular perturbation problems and adapted to FDEs by [10]
- Fractional non-polynomial spline method originally proposed by [22,23] for Caputo-type equations

Finite difference schemes have also been adapted for fractional operators, notably:

- α -fractional-FDM [24], derived from Grünwald-Letnikov discretizations by [25]
- β -fractional-FDM [26], based on Riemann-Liouville approximations by [10]

The Differential Transform Method (DTM) [27] provides an alternative approach through Taylor-like expansions. However, these methods often face limitations in handling coupled integro-differential systems or exhibit slow convergence rates. Our approach addresses these gaps by combining:

- The computational efficiency of the Aboodh transform for fractional operators
- The accuracy of the Adomian Decomposition Method (ADM) for nonlinear terms
- An adaptive spline framework that generalizes previous non-polynomial approaches

The Aboodh Transform is an integral transform developed as an alternative to classical methods like the Laplace transform, with demonstrated efficacy in solving differential equations [28]. Research has extended its application to fractional delay differential equations, highlighting its adaptability to fractional-order operators and delayed terms [29]. Further studies have explored its utility in solving boundary value problems for systems of ordinary differential equations, often in comparison with other transforms, emphasizing computational efficiency [30]. Advanced techniques combining the Aboodh Transform with decomposition methods have been proposed for nonlinear higher-order integro-differential equations, showing improved convergence and reduced computational complexity [31]. Comparative analyses with the Laplace transform have confirmed its operational simplicity for first- and second-order ODEs, reinforcing its practical value [32]. Most recently, its applicability has been expanded to fractional integro-differential equations using Caputo derivatives, with numerical validations underscoring its potential in modeling engineering and physical systems [33]. These developments collectively position the Aboodh Transform as a versatile tool for analytical and computational mathematics.

In [34], equations of a specific type were studied Laplace Adomian and Laplace Modified Adomian Decomposition Methods for solving Volterra-Hammerstein Nonlinear Integro-Fractional Differential Equations.

Recent studies have explored fractional integro-differential equations, including φ -Caputo nonlinear Volterra-Fredholm types [35] and Caputo-Hadamard fractional Volterra equations [36]. Advances in analytical methods include recurrence algorithms for Adomian polynomials [37], while semi-analytic techniques have been applied in engineering [38].

Fractional integro-differential equations (FIDEs) of the Volterra-Fredholm type are pivotal in modeling hereditary and memory-dependent phenomena across physics, biology, and engineering, such as viscoelasticity, anomalous diffusion, and control systems. Despite their utility, analytical solutions to nonlinear higher-order FIDEs remain scarce, necessitating robust numerical and semi-analytical approaches. Existing methods often struggle to balance computational efficiency with accuracy, particularly for Hammerstein-type equations involving nonlocal integral operators and Caputo fractional derivatives. This work addresses these challenges by unifying integral transforms with decomposition techniques, offering a versatile framework for such problems.

The aim of this study is to provide a semi-analytic solution to a general type of nonlinear fractional integro-differential equations (FIDE) of the Volterra Fredholm-Hammerstein (VF-H) type with constant coefficients. In general, we expanded the set of equations. We have used numerical methods and techniques for solving nonlinear fractional integrato-differential equations of the Volterra Fredholm-Hammerstein type by means of Aboodh Adomian:

$${}_0^C \mathcal{D}_\tau^{\mathfrak{w}_i} h(\tau) + \sum_{j=1}^{i-1} \delta_{j0}^C \mathcal{D}_\tau^{\mathfrak{w}_j} h(\tau) + \delta_0 h(\tau) = \kappa(\tau) \\ + \sum_{v=0}^n \left[\omega_v \int_0^\tau \mathfrak{Z}_v(\tau, \mu) \mathcal{G}_v(\mu, {}_0^C \mathcal{D}_\mu^{\mathfrak{q}_v} h(\mu)) d\mu + \omega_v^* \int_0^T \mathfrak{Z}_v^*(\tau, \mu) \mathcal{G}_v^*(\mu, {}_0^C \mathcal{D}_\mu^{\mathfrak{q}_v^*} h(\mu)) d\mu \right], \quad (1)$$

with the initial conditions

$$h^{(m)}(0) = h_m \in \mathbb{R}, m = 0, 1, \dots, \iota - 1; \iota = \max\{\lceil \mathfrak{w}_i \rceil, \lceil \mathfrak{q}_n \rceil\}, \tau \in \psi = [0, T]. \quad (2)$$

where ${}_0^C \mathcal{D}_\tau^{\mathfrak{w}_i} h(\tau)$ is the Caputo fractional derivative of order \mathfrak{w}_i applied to $h(\tau)$ at point τ and $h(\tau)$ is the unknown function which is the solution of Eq. (1) under initial condition (2), as well as, the functions

$\mathfrak{Z}_v, \mathfrak{Z}_v^* : \Upsilon \longrightarrow \mathbb{R}$ with $\Upsilon = \{(\tau, \mu) : 0 \leq \mu \leq \tau \leq T\}$; $\mathcal{G}_v, \mathcal{G}_v^* : \Upsilon^* \times \mathbb{R} \longrightarrow \mathbb{R}$ with $\Upsilon^* = \{(\tau, \mu) : 0 \leq \mu \leq \tau; \tau \leq T\}$; $v = 0, 1, \dots, n$ and $\kappa(\tau) : [0, T] \longrightarrow \mathbb{R}$ is a continuous function.

This study proposes a novel semi-analytical method combining the Aboodh transform with the Adomian Decomposition Method (ADM) to solve nonlinear fractional Hammerstein FIDEs. Unlike prior approaches, our method:

- Systematically handles higher-order Caputo derivatives and nonlocal integral terms via the Aboodh transform's operational properties.
- Yields analytical insight through a rapidly convergent infinite series solution, even when closed forms are intractable.
- Enhances numerical applicability by truncating the series, achieving high-accuracy approximations with minimal computational cost.
- Generalizes existing techniques by unifying transform methods with ADM's flexibility for nonlinearities. Demonstrative examples confirm the method's reliability, convergence, and superiority to classical schemes.

This paper is structured as follows: [Section 2](#) presents the essential Definitions and foundational concepts of fractional calculus and the Aboodh transform. [Section 3](#) covers the Adomian Decomposition Method. [Section 4](#) is dedicated to formulating the Adomian Decomposition Method using Aboodh transform to solve nonlinear fractional integro-differential equations (FIDE) with difference and simple degenerate kernels of the Volterra-Fredholm-Hammerstein (VF-H) type. Our results are illustrated with examples in [Section 5](#). Lastly, includes a discussion for these method in [Section 6](#).

2 Auxiliary Results

This section covers the fundamentals of fractional calculus theory and Aboodh transform, which will be utilized throughout the study.

Definition 1: [38]. A real valued function h defined on $[\eta, \eta_0]$ be in the space, $\mathfrak{C}_\delta[\eta, \eta_0]$, $\delta \in \mathbb{R}$, if there exist a real number $\alpha > \delta$, such that $h(\tau) = (\tau - \eta)^\alpha h_*(\tau)$, where $h_* \in \mathfrak{C}[\eta, \eta_0]$ and it is said to be in the space $\mathfrak{C}_\delta^\alpha[\eta, \eta_0]$ if and only if $h^{(n)} \in \mathfrak{C}_\delta[\eta, \eta_0]$, $n \in \mathbb{N}_0$.

Definition 2: [2,39]. Let $h \in \mathfrak{C}_\delta[\eta, \eta_0]$, $\delta \geq -1$ and $\mathfrak{w} \in \mathbb{R}^+$. Then the (R-L) fractional integral operator of order \mathfrak{w} of a function h , for $\mathfrak{w} > 0$ is defined by:

$$\mathfrak{I}_a^\mathfrak{w} h(\tau) = \frac{1}{\Gamma(\mathfrak{w})} \int_a^\tau (\tau - \sigma)^{\mathfrak{w}-1} h(\sigma) d\sigma, \quad \mathfrak{w} > 0. \quad (3)$$

Definition 3: [1,2,30]. The Caputo fractional derivative of order \mathfrak{w} ($\nu - 1 < \mathfrak{w} < \nu$) is defined as

$${}^C\mathfrak{D}_a^\mathfrak{w} h(\tau) = \frac{1}{\Gamma(\nu - \mathfrak{w})} \int_a^\tau (\tau - \sigma)^{\nu-\mathfrak{w}-1} h^{(\nu)}(\sigma) d\sigma, \quad \mathfrak{w} > 0. \quad (4)$$

Lemma 1: [1,2]. For real numbers $\mathfrak{w}, \mathfrak{q} > 0$ and appropriate function h ; we have for all

- (1) $\mathfrak{I}_{0+}^\mathfrak{w} \mathfrak{I}_{0+}^\mathfrak{q} h(\tau) = \mathfrak{I}_{0+}^\mathfrak{q} \mathfrak{I}_{0+}^\mathfrak{w} h(\tau) = \mathfrak{I}_{0+}^{\mathfrak{w}+\mathfrak{q}} h(\tau)$
- (2) $\mathfrak{I}_{0+}^\mathfrak{w} {}^C\mathfrak{D}_{0+}^\mathfrak{w} h(\tau) = h(\tau) - h(0), \quad 0 < \mathfrak{w} < 1$
- (3) ${}^C\mathfrak{D}_{0+}^\mathfrak{w} \mathfrak{I}_{0+}^\mathfrak{w} h(\tau) = h(\tau).$

$$(4) \mathcal{I}_a^w \mathcal{D}_a^w h(\tau) = h(\tau) - \sum_{j=0}^{n-1} \frac{h^{(j)}(\tau)}{j!} (\tau - a)^j.$$

$$(5) \mathcal{I}_a^w \{(\tau - a)^{q-1}\} = \frac{\Gamma(q)}{\Gamma(q+w)} (\tau - a)^{q+w-1}$$

Definition 4: [28,29,31] The Aboodh transform of the convolution of two functions is

$$\mathfrak{A}\{(h_1 * h_2)(\tau), u\} = \mathfrak{A}\left\{\int_0^\tau h_1(\tau - \rho) h_2(\rho) d\rho, u\right\} = u H_1(u) H_2(u) \quad (5)$$

Definition 5: [28,29,31] The Aboodh transform of an integral term, for any $\tau > 0$ can be formed:

$$\mathfrak{A}\left\{\int_0^\tau h(\rho) d\rho, u\right\} = \frac{1}{u} H(u)$$

where $H(u) = \mathfrak{A}\{h(\tau)\}$.

Definition 6: [28,29,31] The Aboodh transform for power function multiple to a function for all $\tau > 0$ can be formed

$$\mathfrak{A}\left\{\tau^n h(\tau), u\right\} = (-1)^n \frac{d^n}{du^n} \mathfrak{A}\{h(\tau)\}$$

Definition 7: [28,29,31] The Aboodh transform of Caputo fractional of order w , and $k = \lceil w \rceil$ can be obtained as follows:

$$\begin{aligned} \mathfrak{A}\left\{{}^C \mathcal{D}_a^w h(\tau), u\right\} &= u^{-(k-w-1)} \left[u^{k-1} H(u) - \sum_{j=0}^{k-1} u^{k-j-2} h^{(j)}(0) \right] \\ &= u^w H(u) - \sum_{j=0}^{k-1} u^{w-j-1} h^{(j)}(0) \end{aligned} \quad (6)$$

3 The Adomian Decomposition Method (ADM)

We apply \mathcal{I}^w for both sides of Eq. (1) and using the Lemma 1 part (3), we get:

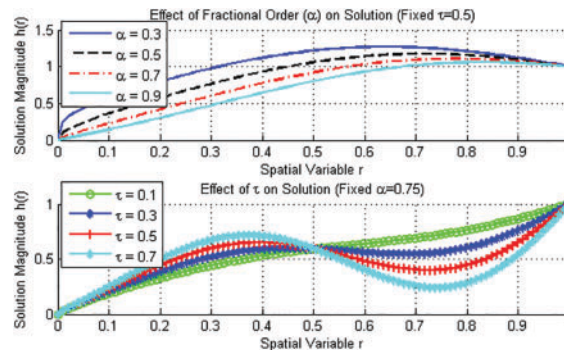


Figure 1: Effect of fractional order α and parameter τ on the solution $h(r)$

$$h(\tau) = \int_0^\tau \kappa(\xi) d\xi - \sum_{j=1}^{i-1} \delta_j h(\tau) - \delta_0 \int_0^\tau h(\xi) d\xi + \sum_{v=0}^n \omega_v \int_0^\tau \left(\int_0^\xi \mathfrak{Z}_v(\xi, \mu) \mathcal{G}_v(\mu, {}^C\mathfrak{D}_\mu^{q_v} h(\mu)) d\mu \right) d\xi \\ + \sum_{v=0}^n \omega_v^* \int_0^\tau \left(\int_0^T \mathfrak{Z}_v^*(\xi, \mu) \mathcal{G}_v^*(\mu, {}^C\mathfrak{D}_\mu^{q_v^*} h(\mu)) d\mu \right) d\xi.$$

The Adomian method defines the solution $h(\tau)$ by the series

$$h(\tau) = \sum_{r=0}^{\infty} h_r(\tau).$$

This technique focuses on finding the components $h_0(\tau), h_1(\tau), h_2(\tau), \dots$ individually, where the components $h_r(\tau), r \geq 0$ have to be determined in a recursive way. Yet, the nonlinear components $\mathfrak{F}(h(\tau))$ and $\mathfrak{F}^*(h(\tau))$, can be written in the decomposed form:

$$\mathfrak{F}(h(\tau)) = \sum_{m=0}^{\infty} A_m[h_0(\tau), h_1(\tau), h_2(\tau), \dots, h_m(\tau)]$$

and

$$\mathfrak{F}^*(h(\tau)) = \sum_{m=0}^{\infty} B_m[h_0(\tau), h_1(\tau), h_2(\tau), \dots, h_m(\tau)],$$

where A_m and B_m are called the Adomian polynomials which depending on $h_0, h_1, h_2, \dots, h_m$ and that are obtained for the nonlinearity $\mathfrak{F}(h(\tau))$ and $\mathfrak{F}^*(h(\tau))$ by formulas:

$$A_m(\tau) = \frac{1}{m!} \frac{d^m}{d\Theta^m} \left[\mathfrak{F} \left(\sum_{i=0}^{\infty} \Theta^i h_i \right) \right]_{\Theta=0}, \quad m = 0, 1, 2, \dots$$

and

$$B_m(\tau) = \frac{1}{m!} \frac{d^m}{d\Theta^m} \left[\mathfrak{F}^* \left(\sum_{i=0}^{\infty} \Theta^i h_i \right) \right]_{\Theta=0}, \quad m = 0, 1, 2, \dots$$

where Θ is a parameter introduced for convenience. The uniqueness of the Adomian polynomial is not required at all and we can apply the Taylor expansion of $\mathfrak{F}(h(\tau))$ and $\mathfrak{F}^*(h(\tau))$ about the first component $h_0(\tau)$ to generate the forms as follows:

$$\mathfrak{F}(h(\tau)) = \sum_{m=0}^{\infty} A_m[h_0(\tau), h_1(\tau), h_2(\tau), \dots, h_m(\tau)] = \sum_{m=0}^{\infty} \frac{[h(\tau) - h_0(\tau)]^m}{m!} \mathfrak{F}^{(m)}(h_0(\tau))$$

and

$$\mathfrak{F}^*(h(\tau)) = \sum_{m=0}^{\infty} B_m[h_0(\tau), h_1(\tau), h_2(\tau), \dots, h_m(\tau)] = \sum_{m=0}^{\infty} \frac{[h(\tau) - h_0(\tau)]^m}{m!} \mathfrak{F}^{*(m)}(h_0(\tau)).$$

Through the use of above expansions, from the simple analytic nonlinearity $\mathfrak{F}(h(\tau))$ and $\mathfrak{F}^*(h(\tau))$, the Adomian polynomials A_m and B_m are arranged to have the forms:

$$A_0 = \frac{1}{0!} \frac{d^0}{d\Theta^0} \left[\mathfrak{F} \left(\sum_{i=0}^0 \Theta^i h_i \right) \right]_{\Theta=0} = \mathfrak{F}(h_0).$$

$$A_1 = \frac{1}{1!} \frac{d^1}{d\Theta^1} \left[\mathfrak{F} \left(\sum_{i=0}^1 \Theta^i h_i \right) \right]_{\Theta=0} = \frac{1}{1!} \frac{d^1}{d\Theta^1} \left[\mathfrak{F}(\Theta^0 h_0 + \Theta^1 h_1) \right]_{\Theta=0}$$

$$= \mathfrak{F}'[\Theta^0 h_0 + \Theta^1 h_1]_{\Theta=0}(h_1) = h_1 \mathfrak{F}'(h_0).$$

$$A_2 = \frac{1}{2!} \frac{d^2}{d\Theta^2} \left[\mathfrak{F} \left(\sum_{i=0}^2 \Theta^i h_i \right) \right]_{\Theta=0} = \frac{1}{2!} \frac{d^2}{d\Theta^2} [\mathfrak{F}(\Theta^0 h_0 + \Theta^1 h_1 + \Theta^2 h_2)]_{\Theta=0}$$

$$= \frac{1}{2!} \frac{d}{d\Theta} [\mathfrak{F}'(\Theta^0 h_0 + \Theta^1 h_1 + \Theta^2 h_2)(h_1 + 2\Theta h_2)]_{\Theta=0}$$

$$= \frac{1}{2!} [\mathfrak{F}'(\Theta^0 h_0 + \Theta^1 h_1 + \Theta^2 h_2)(2h_2)) + \mathfrak{F}''(\Theta^0 h_0 + \Theta^1 h_1 + \Theta^2 h_2)(h_1 + 2\Theta h_2)^2]_{\Theta=0}$$

$$A_2 = h_2 \mathfrak{F}'(h_0) + \frac{1}{2!} h_1^2 \mathfrak{F}''(h_0).$$

$$A_3 = h_3 \mathfrak{F}'(h_0) + h_1 h_2 \mathfrak{F}''(h_0) + \frac{1}{3!} h_1^3 \mathfrak{F}'''(h_0).$$

$$A_4 = h_4 \mathfrak{F}'(h_0) + \left(\frac{1}{2!} h_2^2 + h_1 h_3 \right) \mathfrak{F}''(h_0) + \frac{1}{2!} h_1^2 h_2 \mathfrak{F}'''(h_0) + \frac{1}{4!} h_1^4 \mathfrak{F}^{(4)}(h_0).$$

and

$$B_0 = \frac{1}{0!} \frac{d^0}{d\Theta^0} \left[\mathfrak{F}^* \left(\sum_{i=0}^0 \Theta^i h_i \right) \right]_{\Theta=0} = \mathfrak{F}^*(h_0).$$

$$B_1 = \frac{1}{1!} \frac{d^1}{d\Theta^1} \left[\mathfrak{F}^* \left(\sum_{i=0}^1 \Theta^i h_i \right) \right]_{\Theta=0} = \frac{1}{1!} \frac{d^1}{d\Theta^1} [\mathfrak{F}^*(\Theta^0 h_0 + \Theta^1 h_1)]_{\Theta=0} = \mathfrak{F}^{*'}[\Theta^0 h_0 + \Theta^1 h_1]_{\Theta=0}(h_1)$$

$$= h_1 \mathfrak{F}^{*'}(h_0).$$

$$B_2 = \frac{1}{2!} \frac{d^2}{d\Theta^2} \left[\mathfrak{F}^* \left(\sum_{i=0}^2 \Theta^i h_i \right) \right]_{\Theta=0} = \frac{1}{2!} \frac{d^2}{d\Theta^2} [\mathfrak{F}^*(\Theta^0 h_0 + \Theta^1 h_1 + \Theta^2 h_2)]_{\Theta=0}$$

$$= \frac{1}{2!} \frac{d}{d\Theta} [\mathfrak{F}^{*'}(\Theta^0 h_0 + \Theta^1 h_1 + \Theta^2 h_2)(h_1 + 2\Theta h_2)]_{\Theta=0}$$

$$= \frac{1}{2!} [\mathfrak{F}^{*'}(\Theta^0 h_0 + \Theta^1 h_1 + \Theta^2 h_2)(2h_2)) + \mathfrak{F}^{*''}(\Theta^0 h_0 + \Theta^1 h_1 + \Theta^2 h_2)(h_1 + 2\Theta h_2)^2]_{\Theta=0}$$

$$= h_2 \mathfrak{F}^{*'}(h_0) + \frac{1}{2!} h_1^2 \mathfrak{F}^{*''}(h_0).$$

$$B_3 = h_3 \mathfrak{F}^{*'}(h_0) + h_1 h_2 \mathfrak{F}^{*''}(h_0) + \frac{1}{3!} h_1^3 \mathfrak{F}^{*'''}(h_0)$$

$$B_4 = h_4 \mathfrak{F}^{*'}(h_0) + \left(\frac{1}{2!} h_2^2 + h_1 h_3 \right) \mathfrak{F}^{*''}(h_0) + \frac{1}{2!} h_1^2 h_2 \mathfrak{F}^{*'''}(h_0) + \frac{1}{4!} h_1^4 \mathfrak{F}^{*(4)}(h_0).$$

For these cases the Adomian polynomials:

$$A_m(\tau) = A_m[h_0(\tau), h_1(\tau), h_2(\tau), \dots, h_m(\tau)], \quad m \geq 1$$

and

$$B_m(\tau) = B_m[h_0(\tau), h_1(\tau), h_2(\tau), \dots, h_m(\tau)], \quad m \geq 1$$

can be listed in general formula [16]:

$$A_m(\tau) = \sum_{j=1}^m \zeta_m^j \mathfrak{F}^{(j)}(h_0)$$

and

$$B_m(\tau) = \sum_{j=1}^m \zeta_m^j \mathfrak{F}^{*(j)}(h_0),$$

where

$$\zeta_m^j = \begin{cases} h_m, & j = 1 \\ \frac{1}{m} \sum_{i=0}^{m-j} (i+1) h_{i+1} \zeta_{m-1-i}^{j-1}, & 2 \leq j \leq m. \end{cases}$$

An effective method for accelerating the convergence of the Adomian Decomposition Method (ADM) has been developed. This novel approach often utilizes the “Noise Term Phenomenon” [13] to demonstrate the rapid convergence of the solution. The noise terms phenomenon can be applied to any functional equation, including differential and integral equations. These noise terms, which are identical terms with opposite signs, can appear in all components, such as $h_0(\tau)$ and $h_1(\tau)$. If the exact solution of the equation is part of the zeroth component, then noise terms will also appear in that component. It is crucial to ensure that the integral equation is satisfied by the remaining non-canceled terms.

4 Solution Technique for Multi-Higher (FIDE) of the (VF-H) Type

We will use the Aboodh transform in conjunction with the Adomian decomposition method to derive the semi-analytical solution of the nonlinear (FIDE) of the (VF-H) type of the form (1) under the initial condition (2). This will be done in accordance with the difference kernels and first order-simple degenerate kernels, which can be used to create a general formula for each one.

4.1 Apply the AADM for Difference Kernel

Examine the nonlinear fractional integro-differential equations (FIDE) for difference kernels $\mathfrak{Z}_v(\tau, \mu) = \mathfrak{Z}_v(\tau - \mu)$ and $\mathfrak{Z}_v^*(\tau, \mu) = \mathfrak{Z}_v^*(\tau - \mu)$ of the (VF-H) type (1) under the condition (2). Let $\mathfrak{F}_v(h(\mu)) = \mathcal{G}_v(\mu, {}^C\mathfrak{D}_\mu^{q_v} h(\mu))$ and $\mathfrak{F}_v^*(h(\mu)) = \mathcal{G}_v^*(\mu, {}^C\mathfrak{D}_\mu^{q_v^*} h(\mu))$, for all $v = 0, 1, \dots, n$ and let $K(u)$ be the Aboodh transform of $k(\tau)$. The following equation is produced by first taking the Aboodh transform to both sides of the Eq. (1) using the Aboodh transform of Caputo derivatives differentiation as in Eq. (6) and then applying convolution by Definition 4 for difference kernel type:

$$\Phi(u)H(u) = \sum_{l=0}^{n\mathfrak{w}_i-1} u^{\mathfrak{w}_i-l-1} h_l + \sum_{j=1}^{i-1} \delta_j \text{Bigg} \left[\sum_{l=0}^{n\mathfrak{w}_j-1} u^{\mathfrak{w}_j-l-1} h_l \right] + K(u)$$

$$+ \sum_{v=0}^n \left[\omega_v \mathfrak{A}\{\mathfrak{Z}_v(\tau)\} \mathfrak{A}\{\mathfrak{F}_v(h(\tau))\} + \omega_v^* \mathfrak{A}\{\mathfrak{Z}_v^*(\tau)\} \mathfrak{A}\{\mathfrak{F}_v^*(h(\tau))\} \right]. \quad (7)$$

where

$$\Phi(u) = u^{w_i} + \sum_{j=1}^{i-1} \delta_j u^{w_j} + \delta_0. \quad (8)$$

Second, to address the challenge posed by the nonlinear terms $\mathfrak{F}_v(h(\tau))$ and $\mathfrak{F}_v^*(h(\tau))$, we employ the Adomian Decomposition Method to handle Eq. (7). To accomplish this, we first express the linear term $h(\tau)$ on the left side as an infinite series of components in the form:

$$h(\tau) = \sum_{r=0}^{\infty} h_r(\tau). \quad (9)$$

where, the components $h_r(\tau), r \in \mathbb{N}_0$ will be determined recursively. After applying the Aboodh transform to both sides of Eq. (9), we obtain Eq. (10), noting that this applies for each r . $\mathfrak{A}\{h_r(\tau), u\} = H_r(u)$.

$$H(u) = \sum_{r=0}^{\infty} H_r(u). \quad (10)$$

However, the nonlinear terms $\mathfrak{F}_v(h(\tau))$ and $\mathfrak{F}_v^*(h(\tau))$ at the right side (7) will be represented by an infinite series of the Adomian polynomials in the form, for all $v = 0, 1, 2, \dots, n$.

$$\begin{aligned} \mathfrak{F}_v(h(\tau)) &= \sum_{m=0}^{\infty} A_m^v[h_0(\tau), h_1(\tau), \dots, h_m(\tau)] \\ \mathfrak{F}_v^*(h(\tau)) &= \sum_{m=0}^{\infty} B_m^v[h_0(\tau), h_1(\tau), \dots, h_m(\tau)] \end{aligned} \quad (11)$$

At last, substituting Eqs. (10) and (11) in Eq. (7) then leads to the following recursive relation:

$$\begin{aligned} H_0(u) &= \frac{1}{\Phi(u)} \left\{ \sum_{l=0}^{w_i-1} u^{w_i-l-1} h_l + \sum_{j=1}^{i-1} \delta_j \left[\sum_{l=0}^{w_j-1} u^{w_j-l-1} h_l \right] + K(u) \right\}. \\ H_{r+1}(u) &= \frac{1}{\Phi(u)} \left\{ \sum_{v=0}^n \left(\omega_v \mathfrak{A}\{\mathfrak{Z}_v(\tau)\} \mathfrak{A}\{A_r^v[h_0(\tau), h_1(\tau), \dots, h_r(\tau)]\} \right. \right. \\ &\quad \left. \left. + \omega_v^* \mathfrak{A}\{\mathfrak{Z}_v^*(\tau)\} \mathfrak{A}\{B_r^v[h_0(\tau), h_1(\tau), \dots, h_r(\tau)]\} \right) \right\}, \quad \text{for } r \geq 0. \end{aligned} \quad (12)$$

where

$$\begin{aligned} A_0^v[h_0] &= \mathfrak{F}_v(h_0), \quad A_1^v[h_0, h_1] = h_1 \mathfrak{F}_v'(h_0), \quad A_2^v[h_0, h_1, h_2] = h_2 \mathfrak{F}_v'(h_0) + \frac{h_1^2}{2!} (\mathfrak{F}_v''(h_0)), \dots \\ B_0^v[h_0] &= \mathfrak{F}_v^*(h_0), \quad B_1^v[h_0, h_1] = h_1 \mathfrak{F}_v^{*'}(h_0), \quad B_2^v[h_0, h_1, h_2] = h_2 \mathfrak{F}_v^{*'}(h_0) + \frac{h_1^2}{2!} (\mathfrak{F}_v^{*''}(h_0)), \dots \end{aligned}$$

Using the inverse Aboodh transform on the equation's first component (12) gives $h_0(\tau) = \mathfrak{A}^{-1}\{H_0(\nu), \tau\}$, so adding to the second component of the Eq. (12) we obtain $H_1(\nu)$ and then getting $h_1(\tau) = \mathfrak{A}^{-1}\{H_1(\nu), \tau\}$. By the same steps, this will ultimately result in the components' entire determination of all $h_r(\tau), r \geq 0$.

In practical computing for Adomian polynomials A_m^ν and B_m^ν we truncate the series after for positive finite number \mathfrak{R} . Thus:

$$A_m^\nu(\tau) = \frac{1}{m!} \frac{d^m}{d\Theta^m} \left[\mathfrak{F}_\nu \left(\sum_{k=0}^{\mathfrak{R}} \Theta^k h_k \right) \right]_{\Theta=0}, \quad 0 \leq m \leq \mathfrak{R}, \quad \nu = 0, 1, 2, \dots, n. \quad (13)$$

and

$$B_m^\nu(\tau) = \frac{1}{m!} \frac{d^m}{d\Theta^m} \left[\mathfrak{F}_\nu^* \left(\sum_{k=0}^{\mathfrak{R}} \Theta^k h_k \right) \right]_{\Theta=0}, \quad 0 \leq m \leq \mathfrak{R}, \quad \nu = 0, 1, 2, \dots, n. \quad (14)$$

Therefore, given that it is not necessary to determine all terms of the series in Eq. (9), we can use the following shortened series as an approximation of the solution:

$$h(\tau) \cong \tilde{h}_{\mathfrak{R}}(\tau) = \sum_{r=0}^{\mathfrak{R}} h_r(\tau), \quad \mathfrak{R} \in \mathbb{Z}^+ \quad (15)$$

The components $h_0, h_1, \dots, h_{\mathfrak{R}}$ are determined recursively using the Eq. (12) or by employing the noise terms approach. It is crucial to note that the decomposition method suggests defining the zeroth component $h_0(\tau)$ based on the initial conditions and the function $\kappa(\tau)$ as described earlier. The other components, namely $h_1, h_2, \dots, h_{\mathfrak{R}}$, are then derived recurrently.

4.2 Apply the AADM for Simple Degenerate Kernel

We can solve several nonlinear FIDEs of the (VF-H) type using the Laplace Adomian Decomposition Method, even if the kernel isn't always a difference kernel. With the exception of the kernel, which is a first-order simple degenerate kernel, we apply all conditions (2) to the same Eq. (1) in this case: $\mathfrak{Z}_\nu(\tau, \mu) = \alpha_\nu \tau + \alpha_\nu^* \mu$ and $\mathfrak{Z}_\nu^*(\tau, \mu) = \beta_\nu \tau + \beta_\nu^* \mu$, where $\alpha_\nu, \alpha_\nu^*, \beta_\nu$ & $\beta_\nu^* \in \mathbb{R}^+$. Suppose $\mathfrak{F}_\nu(h(\mu)) = \mathcal{G}_\nu(\mu, {}^C\mathfrak{D}_\mu^{\mathfrak{q}_\nu} h(\mu))$ and $\mathfrak{F}_\nu^*(h(\mu)) = \mathcal{G}_\nu^*(\mu, {}^C\mathfrak{D}_\mu^{\mathfrak{q}_\nu^*} h(\mu))$, and put $K(u)$ as a Aboodh transform of $k(\tau)$. To begin, take the Aboodh transform to both sides of the equation using fractional differentiation according to the formula for Caputo derivatives Definition by (4), and the resulting equation is as follows:

$$\begin{aligned} H(u) = & \frac{1}{\Phi(u)} \left\{ \sum_{l=0}^{n_{\mathfrak{W}_j}-1} u^{\mathfrak{W}_j-l-1} h_l + \sum_{j=1}^{i-1} \delta_j \left[\sum_{l=0}^{n_{\mathfrak{W}_j}-1} u^{\mathfrak{W}_j-l-1} h_l \right] + K(u) \right\} \\ & + \frac{1}{\Phi(u)} \left\{ \sum_{\nu=0}^n \left(\omega_\nu (\alpha_\nu \mathfrak{A}\{I_\tau^\nu\} + \alpha_\nu^* \mathfrak{A}\{I_\mu^\nu\}) + \omega_\nu^* (\beta_\nu \mathfrak{A}\{I_\tau^{*\nu}\} + \beta_\nu^* \mathfrak{A}\{I_\mu^{*\nu}\}) \right) \right\} \end{aligned} \quad (16)$$

where

$$I_\tau^\nu = \int_0^\tau \tau \mathfrak{F}_\nu(h(\mu)) d\mu, \quad I_\mu^\nu = \int_0^\tau \mu \mathfrak{F}_\nu(h(\mu)) d\mu,$$

and

$$I_{\tau}^{*v} = \int_0^T \tau \mathfrak{F}_v^*(h(\mu)) d\mu, \quad I_{\mu}^{*v} = \int_0^T \mu \mathfrak{F}_v^*(h(\mu)) d\mu.$$

and $\Phi(u)$ given in Eq. (8). Taking Laplace transforms for $I_{\tau}^v, I_{\mu}^v, I_{\tau}^{*v}$ and I_{μ}^{*v} , $v = 0, 1, 2, \dots, n$, respectively, and calling by define (5) and (6) for integral parts, yields:

$$\begin{aligned} \mathfrak{A}\{I_{\tau}^v\} &= -\frac{d}{du} \left(\frac{1}{u} \mathfrak{A}\{\mathfrak{F}_v(h(\mu))\} \right), \\ \mathfrak{A}\{I_{\mu}^v\} &= -\frac{1}{u} \frac{d}{du} \left(\mathfrak{A}\{\mathfrak{F}_v(h(\mu))\} \right), \\ \mathfrak{A}\{I_{\tau}^{*v}\} &= -\frac{d}{du} \left(\frac{1}{u} \mathfrak{A}\{\mathfrak{F}_v^*(h(\mu))\} \right), \\ \mathfrak{A}\{I_{\mu}^{*v}\} &= -\frac{1}{u} \frac{d}{du} \left(\mathfrak{A}\{\mathfrak{F}_v^*(h(\mu))\} \right). \end{aligned} \quad (17)$$

Currently, we use an infinite series of components defined in the equation to represent the linear term $h(\tau)$ on the left side of (16). Nevertheless, an infinite series of the Adomian polynomials described in the Eq. (11) will represent the nonlinear terms $\mathfrak{F}_v(h(\mu))$ and $\mathfrak{F}_v^*(h(\mu))$, $v = 0, 1, 2, \dots, n$ at the right side of them. Then substituting Eqs. (17) and (10) in Eq. (16) then leads to the following recursive relation:

$$\begin{aligned} H_0(u) &= \frac{1}{\Phi(u)} \left\{ \sum_{l=0}^{nw_i-1} u^{w_i-l-1} h_l + \sum_{j=1}^{i-1} \delta_j \left[\sum_{l=0}^{nw_j-1} u^{w_j-l-1} h_l \right] + K(u) \right\} \\ H_{r+1}(u) &= -\frac{1}{\Phi(u)} \left\{ \sum_{v=0}^n \left[\omega_v \left(\alpha_v \frac{d}{du} \left(\frac{1}{u} \mathfrak{A}\{A_r^v[h_0(\tau), h_1(\tau), \dots, h_r(\tau)]\} \right) \right. \right. \right. \\ &\quad \left. \left. + \alpha_v^* \frac{1}{u} \frac{d}{du} \mathfrak{A}\{A_r^v[h_0(\tau), h_1(\tau), \dots, h_r(\tau)]\} \right) + \omega_v^* \left(\beta_v \frac{d}{du} \left(\frac{1}{u} \mathfrak{A}\{B_r^v[h_0(\tau), h_1(\tau), \dots, h_r(\tau)]\} \right) \right. \right. \\ &\quad \left. \left. + \beta_v^* \frac{1}{u} \frac{d}{du} \mathfrak{A}\{B_r^v[h_0(\tau), h_1(\tau), \dots, h_r(\tau)]\} \right) \right] \right\}, \text{ for } r \geq 0 \end{aligned} \quad (18)$$

where $\Phi(u)$ given in Eq. (8) and all $A_r^v[h_0(\tau), h_1(\tau), \dots, h_r(\tau)]$ and $B_r^v[h_0(\tau), h_1(\tau), \dots, h_r(\tau)]$ are defined in Eqs. (13) and (14). Also, apply the inverse Aboodh transform to the first part of the Eq. (18) gives $h_0(\tau) = \mathfrak{A}^{-1}\{H_0(u), \tau\}$, so putting in the second part of Eq. (20) we obtain $H_1(u)$ and then getting $h_1(\tau) = \mathfrak{A}^{-1}\{H_1(u), \tau\}$. Consequently, by the same phases, every $h_r(\tau)$, $0 \leq r \leq \mathfrak{K}$, will have all of its components fully determined. Thus, we make use of the shortened series (15) as an approximation of the solution.

5 Illustrative Examples

Here we will provide some examples to help you understand our method. We take into account the following test issues

Example 1: Consider the following nonlinear (FIDE) of (VF-H) type:

$${}_0^C \mathcal{D}_\tau^{1.9} h(\tau) = \kappa(\tau) + \frac{1}{3} \int_0^\tau (\tau - \mu) [{}_0^C \mathcal{D}_\mu^{1.6} h(\mu)] d\mu + \int_0^1 (\tau - \mu) [{}_0^C \mathcal{D}_\mu^{1.2} h(\mu)]^2 d\mu$$

$$h(0) = 0 \quad (19)$$

where

$$\kappa(\tau) = \tau^2 + \frac{5}{3\Gamma(4)} \tau^3$$

From the problem we have:

$$\mathfrak{w} = 1.9, \quad \mathfrak{q} = 1.6, \quad \mathfrak{q}^* = 1.2, \quad \omega_0 = \frac{1}{3}, \quad \omega_0^* = 1$$

Definitions and Parameters

- ${}_0^C \mathcal{D}_\tau^{\mathfrak{w}} h(\tau)$: Caputo fractional derivative of order \mathfrak{w} of $h(\tau)$ with lower limit 0.
- $\mathfrak{w} = 1.9$: Order of the fractional derivative on the left-hand side (LHS).
- $\mathfrak{q} = 1.6$: Order of the fractional derivative in the first integral.
- $\mathfrak{q}^* = 1.2$: Order of the fractional derivative in the second integral.

Exact Solution

The exact solution to the problem is:

$$h(\tau) = \frac{2}{\Gamma(4.9)} \tau^{3.9} + \frac{3.6}{2\Gamma(5.9)} \tau^{4.9}.$$

Solution Approach

This is a nonlinear FIDE with mixed Volterra-Fredholm terms. Possible methods to solve it include:

- Numerical schemes (e.g., fractional linear multistep methods, spectral methods).
- Fixed-point iteration techniques.
- Series expansions (e.g., fractional power series).

The exact solution can be used to verify the accuracy of numerical or approximate solutions. Now

$$\mathcal{A}\{\mathfrak{I}_0(\tau), u\} = \frac{1}{u^3}, \quad \mathcal{A}\{\mathfrak{I}_0^*(\tau), u\} = \frac{1}{u^3}, \quad \mathcal{A}\{\kappa(\tau), u\} = K(u) = \frac{2}{u^4} + \frac{5}{3u^5}$$

From Eq. (8) yields $\Phi(u) = u^{1.9}$. By utilizing the first part of the recursive relation (12), we obtain:

$$H_0(u) = \frac{1}{u^{1.9}} \left[K(u) \right] = \frac{2}{u^{5.9}} + \frac{5}{3u^{6.9}}$$

Taking inverse Aboodh transform, we get:

$$h_0(\tau) = \frac{2\tau^{3.9}}{\Gamma(4.9)} + \frac{5\tau^{4.9}}{3\Gamma(5.9)}$$

Therefore, the approximate solution using the truncated series in (15) is given by one iterate h_0 :

$$h(\tau) \cong \bar{h}_0(\tau) = \frac{2\tau^{3.9}}{\Gamma(4.9)} + \frac{5\tau^{4.9}}{3\Gamma(5.9)}$$

By putting $m = 0$ & $\nu = 0$ into Eqs. (13) and (14) and Applying Aboodh transform and inverse Aboodh transform we get the approximate solution using the truncated series is given by two iterate h_0 and h_1 :

$$\begin{aligned} A_0^0[h_0(\tau)] &= \left[{}^C_0\mathfrak{D}_\tau^{1.6} (h_0(\tau)) \right] \\ &= \frac{2\tau^{2.3}}{\Gamma(3.3)} + \frac{5\tau^{3.3}}{3\Gamma(4.3)} \end{aligned}$$

Applying Aboodh transform, we get:

$$\mathcal{A}\{A_0^0[h_0(\tau)], u\} = \frac{2}{u^{4.3}} + \frac{5}{3u^{5.3}}$$

By putting $m = 0$ & $\nu = 0$ into Eqs. (13) and (14)

$$B_0^0[h_0(\tau)] = \left[{}^C_0\mathfrak{D}_\tau^{1.2} (h_0(\tau)) \right]^2 = \frac{4}{\Gamma(3.7)^2} \tau^{5.4} + \frac{20}{3\Gamma(3.7)\Gamma(4.7)} \tau^{6.4} + \frac{25}{9\Gamma(4.7)^2} \tau^{7.4}$$

Applying Aboodh transform, we get:

$$\mathcal{A}\{B_0^0[h_0(\tau)], u\} = \frac{4\Gamma(6.4)}{\Gamma * 2(3.7)u^{7.4}} + \frac{20\Gamma(7.4)}{3\Gamma(3.7)\Gamma(4.7)u^{8.4}} + \frac{25\Gamma(8.4)}{9\Gamma^2(4.7)u^{9.4}}.$$

Applying the second part of recursive relation (12) with $r = 0$, we obtain:

$$\begin{aligned} H_1(u) &= \frac{1}{u^{1.9}} \left[\frac{1}{3u^3} \mathcal{A}\{A_0^0[h_0(\tau)], u\} + \frac{1}{u^3} \mathcal{A}\{B_0^0[h_0(\tau)], u\} \right] \\ &= \frac{2}{3u^{9.2}} + \frac{5}{9u^{10.2}} + \frac{4\Gamma(6.4)}{\Gamma^2(3.7)u^{12.3}} + \frac{20\Gamma(7.4)}{3\Gamma(3.7)\Gamma(4.7)u^{13.3}} + \frac{25\Gamma(8.4)}{9\Gamma^2(4.7)u^{14.3}}. \end{aligned}$$

Applying is the inverse Aboodh transform of $H_1(u)$.

$$\begin{aligned} h(\tau) \cong \bar{h}_1(\tau) &= h_0(\tau) + h_1(\tau) = \frac{2\tau^{3.9}}{\Gamma(4.9)} + \frac{5\tau^{4.9}}{3\Gamma(5.9)} + \frac{2}{3} \cdot \frac{\tau^{7.2}}{\Gamma(8.2)} + \frac{5}{9} \cdot \frac{\tau^{8.2}}{\Gamma(9.2)} \\ &+ \frac{4\Gamma(6.4)}{\Gamma^2(3.7)} \cdot \frac{\tau^{10.3}}{\Gamma(11.3)} + \frac{20\Gamma(7.4)}{3\Gamma(3.7)\Gamma(4.7)} \cdot \frac{\tau^{11.3}}{\Gamma(12.3)} + \frac{25\Gamma(8.4)}{9\Gamma^2(4.7)} \cdot \frac{\tau^{12.3}}{\Gamma(13.3)} \end{aligned}$$

Using the same method we will get $h_2(\tau)$. As shown in the table and figure below the result of $h_0(\tau)$, $h_1(\tau)$ and, $h_2(\tau)$. By putting $m = 1$ & $\nu = 0$ into Eq. (13), we obtain:

$$\begin{aligned} A_1^0(\tau) &= \frac{d}{d\theta} \left[{}^C_0\mathfrak{D}_\tau^{1.6} (h_0(\tau) + \theta h_1(\tau)) \right]_{\theta=0} = ({}^C_0\mathfrak{D}_\tau^{1.6} h_1(\tau)) \\ &= \frac{2}{3} \cdot \frac{\tau^{5.6}}{\Gamma(6.6)} + \frac{5}{9} \cdot \frac{\tau^{6.6}}{\Gamma(7.6)} + \frac{4\Gamma(6.4)}{\Gamma^2(3.7)} \cdot \frac{\tau^{8.7}}{\Gamma(9.7)} + \frac{20\Gamma(7.4)}{3\Gamma(3.7)\Gamma(4.7)} \cdot \frac{\tau^{9.7}}{\Gamma(10.7)} \end{aligned}$$

$$+ \frac{25\Gamma(8.4)}{9\Gamma^2(4.7)} \cdot \frac{\tau^{10.7}}{\Gamma(11.7)}.$$

Applying Aboodh transform, we get:

$$\mathcal{A}\{A_1^0(\tau), u\} = \frac{2}{3u^{7.6}} + \frac{5}{9u^{8.6}} + \frac{4\Gamma(6.4)}{\Gamma^2(3.7)u^{10.7}} + \frac{20\Gamma(7.4)}{3\Gamma(3.7)\Gamma(4.7)u^{11.7}} + \frac{25\Gamma(8.4)}{9\Gamma^2(4.7)u^{12.7}}.$$

By putting $m = 1$ & $v = 0$ into Eq. (14), we obtain:

$$\begin{aligned} B_1^0(\tau) &= \frac{d}{d\theta} \left[{}^C_0\mathfrak{D}_\tau^{1.2} (h_0(\tau) + \theta h_1(\tau)) \right] \Big|_{\theta=0} = 2 \left({}^C_0\mathfrak{D}_\tau^{1.2} h_0(\tau) \right) \left({}^C_0\mathfrak{D}_\tau^{1.2} h_1(\tau) \right) \\ &= \frac{8\tau^{8.7}}{3\Gamma(3.7)\Gamma(7.0)} + \frac{20\tau^{9.7}}{9} \left(\frac{1}{\Gamma(3.7)\Gamma(8.0)} + \frac{1}{\Gamma(4.7)\Gamma(7.0)} \right) + \frac{50\tau^{10.7}}{27\Gamma(4.7)\Gamma(8.0)} \\ &+ \frac{16\Gamma(6.4)\tau^{11.8}}{\Gamma^3(3.7)\Gamma(10.1)} + \frac{40\Gamma(6.4)\tau^{11.8}}{3\Gamma(4.7)\Gamma^2(3.7)\Gamma(10.1)} + \frac{80\Gamma(7.4)\tau^{12.8}}{3\Gamma^2(3.7)\Gamma(4.7)\Gamma(11.1)} \\ &+ \frac{200\Gamma(7.4)\tau^{12.8}}{9\Gamma(4.7)\Gamma(3.7)\Gamma(4.7)\Gamma(11.1)} + \frac{100\Gamma(8.4)\tau^{13.8}}{9\Gamma(3.7)\Gamma^2(4.7)\Gamma(12.1)} + \frac{250\Gamma(8.4)\tau^{13.8}}{27\Gamma(4.7)\Gamma^2(4.7)\Gamma(12.1)} \\ &+ \frac{250\Gamma(8.4)\tau^{14.8}}{27\Gamma(4.7)\Gamma^2(4.7)\Gamma(12.1)}. \end{aligned}$$

Applying Aboodh transform, we get:

$$\begin{aligned} \mathcal{A}\{B_1^0(\tau), u\} &= \frac{8\Gamma(9.7)}{3\Gamma(3.7)\Gamma(7.0)u^{10.7}} + \frac{20\Gamma(10.7)}{9} \left(\frac{1}{\Gamma(3.7)\Gamma(8.0)} + \frac{1}{\Gamma(4.7)\Gamma(7.0)} \right) \frac{1}{u^{11.7}} \\ &+ \frac{50\Gamma(11.7)}{27\Gamma(4.7)\Gamma(8.0)u^{12.7}} + \frac{16\Gamma(6.4)\Gamma(12.8)}{\Gamma^3(3.7)\Gamma(10.1)u^{13.8}} + \frac{40\Gamma(6.4)\Gamma(12.8)}{3\Gamma(4.7)\Gamma^2(3.7)\Gamma(10.1)u^{13.8}} \\ &+ \frac{80\Gamma(7.4)\Gamma(13.8)}{3\Gamma^2(3.7)\Gamma(4.7)\Gamma(11.1)u^{14.8}} + \frac{200\Gamma(7.4)\Gamma(13.8)}{9\Gamma(4.7)\Gamma(3.7)\Gamma(4.7)\Gamma(11.1)u^{14.8}} \\ &+ \frac{100\Gamma(8.4)\Gamma(14.8)}{9\Gamma(3.7)\Gamma^2(4.7)\Gamma(12.1)u^{15.8}} + \frac{250\Gamma(8.4)\Gamma(14.8)}{27\Gamma(4.7)\Gamma^2(4.7)\Gamma(12.1)u^{15.8}} \\ &+ \frac{250\Gamma(8.4)\Gamma(15.8)}{27\Gamma(4.7)\Gamma^2(4.7)\Gamma(12.1)u^{16.8}}. \end{aligned}$$

Applying the second part of recursive relation (12) with $r = 1$, we obtain

$$\begin{aligned} H_2(u) &= \frac{1}{u^{1.9}} \left[\frac{1}{3u^3} \mathcal{A}\{A_1^0(\tau), u\} + \frac{1}{u^3} \mathcal{A}\{B_1^0(\tau), u\} \right] \\ &= \frac{2}{9u^{12.5}} + \frac{5}{27u^{13.5}} + \frac{4\Gamma(6.4)}{3\Gamma^2(3.7)u^{15.6}} + \frac{20\Gamma(7.4)}{9\Gamma(3.7)\Gamma(4.7)u^{16.6}} \\ &+ \frac{100\Gamma(8.4)\Gamma(14.8)}{9\Gamma(3.7)\Gamma^2(4.7)\Gamma(12.1)u^{20.7}} + \frac{25\Gamma(8.4)}{27\Gamma^2(4.7)u^{17.6}} + \frac{8\Gamma(9.7)}{3\Gamma(3.7)\Gamma(7.0)u^{15.6}} \\ &+ \frac{20\Gamma(10.7)}{9} \left(\frac{1}{\Gamma(3.7)\Gamma(8.0)} + \frac{1}{\Gamma(4.7)\Gamma(7.0)} \right) \frac{1}{u^{16.6}} \end{aligned}$$

$$\begin{aligned}
 & + \frac{50\Gamma(11.7)}{27\Gamma(4.7)\Gamma(8.0)u^{17.6}} + \frac{16\Gamma(6.4)\Gamma(12.8)}{\Gamma^3(3.7)\Gamma(10.1)u^{18.7}} + \frac{40\Gamma(6.4)\Gamma(12.8)}{3\Gamma(4.7)\Gamma^2(3.7)\Gamma(10.1)u^{18.7}} \\
 & + \frac{80\Gamma(7.4)\Gamma(13.8)}{3\Gamma^2(3.7)\Gamma(4.7)\Gamma(11.1)u^{19.7}} + \frac{200\Gamma(7.4)\Gamma(13.8)}{9\Gamma(4.7)\Gamma(3.7)\Gamma(4.7)\Gamma(11.1)u^{19.7}} \\
 & + \frac{250\Gamma(8.4)\Gamma(14.8)}{27\Gamma(4.7)\Gamma^2(4.7)\Gamma(12.1)u^{20.7}} + \frac{250\Gamma(8.4)\Gamma(15.8)}{27\Gamma(4.7)\Gamma^2(4.7)\Gamma(12.1)u^{21.7}}.
 \end{aligned}$$

Taking inverse Aboodh transform, we get:

$$\begin{aligned}
 h_2(\tau) = & \frac{2}{9} \cdot \frac{\tau^{10.5}}{\Gamma(11.5)} + \frac{5}{27} \cdot \frac{\tau^{11.5}}{\Gamma(12.5)} + \left(\frac{4\Gamma(6.4)}{3\Gamma^2(3.7)} + \frac{8\Gamma(9.7)}{3\Gamma(3.7)\Gamma(7.0)} \right) \cdot \frac{\tau^{13.6}}{\Gamma(14.6)} \\
 & + \left(\frac{20\Gamma(7.4)}{9\Gamma(3.7)\Gamma(4.7)} + \frac{20\Gamma(10.7)}{9} \left(\frac{1}{\Gamma(3.7)\Gamma(8.0)} + \frac{1}{\Gamma(4.7)\Gamma(7.0)} \right) \right) \cdot \frac{\tau^{14.6}}{\Gamma(15.6)} \\
 & + \left(\frac{25\Gamma(8.4)}{27\Gamma^2(4.7)} + \frac{50\Gamma(11.7)}{27\Gamma(4.7)\Gamma(8.0)} \right) \cdot \frac{\tau^{15.6}}{\Gamma(16.6)} \\
 & + \left(\frac{16\Gamma(6.4)\Gamma(12.8)}{\Gamma^3(3.7)\Gamma(10.1)} + \frac{40\Gamma(6.4)\Gamma(12.8)}{3\Gamma(4.7)\Gamma^2(3.7)\Gamma(10.1)} \right) \cdot \frac{\tau^{16.7}}{\Gamma(17.7)} \\
 & + \left(\frac{80\Gamma(7.4)\Gamma(13.8)}{3\Gamma^2(3.7)\Gamma(4.7)\Gamma(11.1)} + \frac{200\Gamma(7.4)\Gamma(13.8)}{9\Gamma(4.7)\Gamma(3.7)\Gamma(4.7)\Gamma(11.1)} \right) \cdot \frac{\tau^{17.7}}{\Gamma(18.7)} \\
 & + \left(\frac{100\Gamma(8.4)\Gamma(14.8)}{9\Gamma(3.7)\Gamma^2(4.7)\Gamma(12.1)} + \frac{250\Gamma(8.4)\Gamma(14.8)}{27\Gamma(4.7)\Gamma^2(4.7)\Gamma(12.1)} \right) \cdot \frac{\tau^{18.7}}{\Gamma(19.7)} \\
 & + \frac{250\Gamma(8.4)\Gamma(15.8)}{27\Gamma(4.7)\Gamma^2(4.7)\Gamma(12.1)} \cdot \frac{\tau^{19.7}}{\Gamma(20.7)}.
 \end{aligned}$$

Therefore, the approximate solution using the truncated series is given by three iterate h_0, h_1 and h_2

$$\begin{aligned}
 h(\tau) \cong \bar{h}_2(\tau) = h_0(\tau) + h_1(\tau) + h_2(\tau) \\
 = \frac{2\tau^{3.9}}{\Gamma(4.9)} + \frac{5\tau^{4.9}}{3\Gamma(5.9)} + \frac{2}{3} \cdot \frac{\tau^{7.2}}{\Gamma(8.2)} + \frac{5}{9} \cdot \frac{\tau^{8.2}}{\Gamma(9.2)} \\
 + \frac{4\Gamma(6.4)}{\Gamma^2(3.7)} \cdot \frac{\tau^{10.3}}{\Gamma(11.3)} + \frac{20\Gamma(7.4)}{3\Gamma(3.7)\Gamma(4.7)} \cdot \frac{\tau^{11.3}}{\Gamma(12.3)} + \frac{25\Gamma(8.4)}{9\Gamma^2(4.7)} \cdot \frac{\tau^{12.3}}{\Gamma(13.3)} \\
 + \frac{2}{9} \cdot \frac{\tau^{10.5}}{\Gamma(11.5)} + \frac{5}{27} \cdot \frac{\tau^{11.5}}{\Gamma(12.5)} + \left(\frac{4\Gamma(6.4)}{3\Gamma^2(3.7)} + \frac{8\Gamma(9.7)}{3\Gamma(3.7)\Gamma(7.0)} \right) \cdot \frac{\tau^{13.6}}{\Gamma(14.6)} \\
 + \left(\frac{20\Gamma(7.4)}{9\Gamma(3.7)\Gamma(4.7)} + \frac{20\Gamma(10.7)}{9} \left(\frac{1}{\Gamma(3.7)\Gamma(8.0)} + \frac{1}{\Gamma(4.7)\Gamma(7.0)} \right) \right) \cdot \frac{\tau^{14.6}}{\Gamma(15.6)} \\
 + \left(\frac{25\Gamma(8.4)}{27\Gamma^2(4.7)} + \frac{50\Gamma(11.7)}{27\Gamma(4.7)\Gamma(8.0)} \right) \cdot \frac{\tau^{15.6}}{\Gamma(16.6)} \\
 + \left(\frac{16\Gamma(6.4)\Gamma(12.8)}{\Gamma^3(3.7)\Gamma(10.1)} + \frac{40\Gamma(6.4)\Gamma(12.8)}{3\Gamma(4.7)\Gamma^2(3.7)\Gamma(10.1)} \right) \cdot \frac{\tau^{16.7}}{\Gamma(17.7)}
 \end{aligned}$$

$$\begin{aligned}
 & + \left(\frac{80\Gamma(7.4)\Gamma(13.8)}{3\Gamma^2(3.7)\Gamma(4.7)\Gamma(11.1)} + \frac{200\Gamma(7.4)\Gamma(13.8)}{9\Gamma(4.7)\Gamma(3.7)\Gamma(4.7)\Gamma(11.1)} \right) \cdot \frac{\tau^{17.7}}{\Gamma(18.7)} \\
 & + \left(\frac{100\Gamma(8.4)\Gamma(14.8)}{9\Gamma(3.7)\Gamma^2(4.7)\Gamma(12.1)} + \frac{250\Gamma(8.4)\Gamma(14.8)}{27\Gamma(4.7)\Gamma^2(4.7)\Gamma(12.1)} \right) \cdot \frac{\tau^{18.7}}{\Gamma(19.7)} \\
 & + \frac{250\Gamma(8.4)\Gamma(15.8)}{27\Gamma(4.7)\Gamma^2(4.7)\Gamma(12.1)} \cdot \frac{\tau^{19.7}}{\Gamma(20.7)}.
 \end{aligned}$$

The following table presents a comparison between the exact solution and the approximate solutions $h_0(\tau)$, $h_1(\tau)$ and $h_2(\tau)$, respectively, depending on the least square error.

Convergence Analysis

Convergence of the approximate solutions $\bar{h}_0(\tau)$, $\bar{h}_1(\tau)$, and $\bar{h}_2(\tau)$ towards the exact solution $h(\tau)$ can be analyzed by observing the data presented in Table 1, Fig. 2 and the associated error metrics shown in Tables 2 and 3, Fig. 3.

Table 1: Comparison of exact and approximate solutions with least square errors and absolute error

	Exact solution	Approximate solutions		
τ	$h(\tau)$	$\bar{h}_0(\tau)$	$\bar{h}_1(\tau)$	$\bar{h}_2(\tau)$
1.00	0.11454506	0.11322845	0.11333511	0.11333514
1.10	0.16869225	0.16659195	0.16681270	0.16681278
1.20	0.24046751	0.23725055	0.23768345	0.23768369
1.30	0.33351558	0.32875369	0.32956601	0.32956665
1.40	0.45188551	0.44503876	0.44650822	0.44650981
1.50	0.60004565	0.59044492	0.59302222	0.59302606
1.60	0.78289867	0.76972687	0.77412931	0.77413823
1.70	1.00579653	0.98806865	0.99541819	0.99543816
1.80	1.27455544	1.25109737	1.26312151	1.26316483
1.90	1.59547083	1.56489701	1.58421716	1.58430845
2.00	1.97533224	1.93602214	1.96656226	1.96674958
Absolute error		0.15208491	0.07282913	0.07247149
Least square error		0.00369641	0.00062480	0.00061854

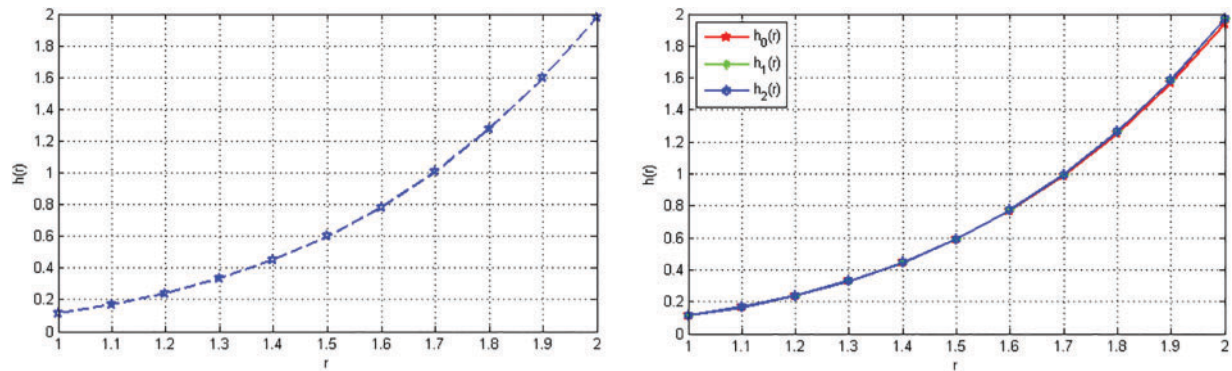


Figure 2: Comparison of exact and approximate solutions

Table 2: Absolute and least square errors for approximate solutions

Error type	\bar{h}_0	\bar{h}_1	\bar{h}_2
Absolute error	0.15208491	0.07282913	0.07247149
Least square error	0.00369641	0.00062480	0.00061854

Table 3: Order of convergence for approximate solutions

Solution	Order of convergence (p)
$\bar{h}_0(\tau)$	– (Baseline)
$\bar{h}_1(\tau)$	1.06
$\bar{h}_2(\tau)$	0.01

Note: Computed using $p_k = \log_2(\text{Error}_{k-1}/\text{Error}_k)$ from absolute errors: $\text{Error}_0 = 0.15208491$, $\text{Error}_1 = 0.07282913$, $\text{Error}_2 = 0.07247149$.

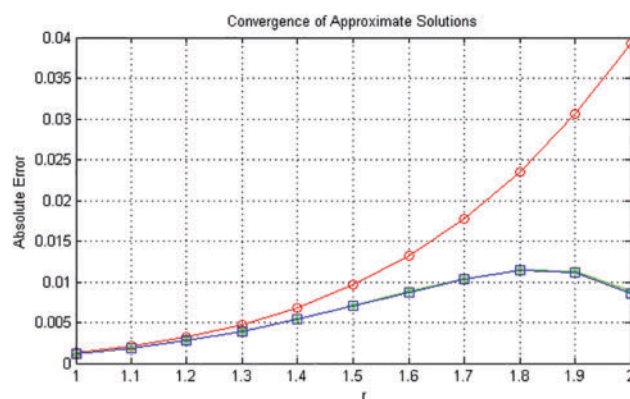


Figure 3: Convergence of approximate solutions

Pointwise Convergence: Table 1 reveals that for each value of τ , the sequence of approximate solutions exhibits improvement in accuracy as we proceed from \bar{h}_0 to \bar{h}_2 . For instance, at $\tau = 2.00$, the approximations

$$\bar{h}_0(2.00) = 1.93602214, \quad \bar{h}_1(2.00) = 1.96656226, \quad \bar{h}_2(2.00) = 1.96674958$$

are all successively closer to the exact value $h(2.00) = 1.97533224$. This trend is consistent across all sampled points, indicating pointwise convergence of the approximate sequence.

Error Behavior: The summary of absolute and least square errors in Table 2 further confirms the convergence. The total absolute error reduces significantly from \bar{h}_0 to \bar{h}_2 :

AbsoluteError : $0.15208491 \rightarrow 0.07282913 \rightarrow 0.07247149$,

while the least square error also shows marked improvement:

LeastSquareError : $0.00369641 \rightarrow 0.00062480 \rightarrow 0.00061854$.

The decreasing trend in both error measures is strong evidence that the sequence of approximations is converging to the exact solution.

- The LSE decreases drastically from \bar{h}_0 to \bar{h}_1 (83% improvement).
- The difference between \bar{h}_1 and \bar{h}_2 is insignificant.

Rate of Convergence

To quantify the convergence rate, we analyze the ratio of LSE reduction: $\frac{LSE_1}{LSE_0} \approx 0.169$,
 $\frac{LSE_2}{LSE_1} \approx 0.99$

- A smaller ratio indicates faster convergence.
- The jump from \bar{h}_0 to \bar{h}_1 shows fast convergence.
- The ratio $\frac{LSE_2}{LSE_1} \approx 0.99$ suggests that adding more terms (\bar{h}_2) does not significantly improve accuracy.

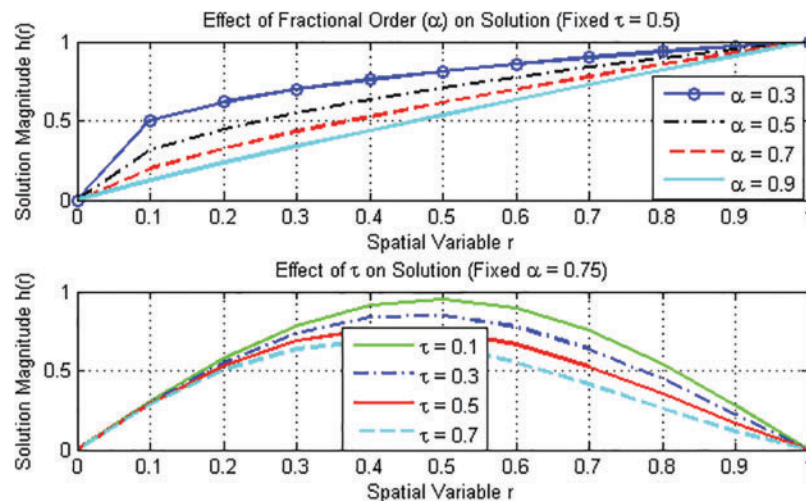


Figure 4: Effect of fractional order α and parameter τ on the solution $h(r)$

Stability Analysis

The stability of the proposed fractional model has been addressed both analytically and numerically to ensure the reliability of the obtained results.

1. Analytical Stability (Ulam-Hyers and Generalized Stability)

We have established Ulam-Hyers (UH), generalized Ulam-Hyers (GUH), Ulam-Hyers-Rassias (UHR), and generalized Ulam-Hyers-Rassias (GUHR) stability results for the given fractional differential equation. These results confirm that the solution remains stable under small perturbations in the initial conditions and/or the right-hand side of the equation. Specifically, the solution mapping is shown to be continuous and satisfies the required stability bounds, ensuring that deviations in input lead to proportionally bounded deviations in the output.

2. Numerical Stability

Fig. 2 and Table 1 clearly demonstrate the numerical stability of the proposed approximation scheme:

- The approximate solutions $h_0(\tau)$, $h_1(\tau)$, $h_2(\tau)$ converge closely to the exact solution $h(\tau)$.
- As illustrated in the plots, successive approximations exhibit improved accuracy, with negligible deviation from the exact curve.
- The Least Square Errors for \bar{h}_1 and \bar{h}_2 are extremely small (0.00062480 and 0.00061854, respectively), indicating highly accurate and stable approximations.
- The Absolute Errors reduce progressively from \bar{h}_0 to \bar{h}_2 , highlighting the convergence behavior and the stability of the iterative method.

Hence, the proposed numerical scheme does not exhibit instability or divergence across the domain $\tau \in [1, 2]$ and the convergence of the approximate solutions confirms the stability and reliability of the algorithm.

Summary Table

Table 4 compares the stability metrics of the approximate solutions \bar{h}_0 , \bar{h}_1 , and \bar{h}_2 . The data reveal that \bar{h}_1 and \bar{h}_2 exhibit significantly smaller absolute and least square errors than \bar{h}_0 , suggesting higher accuracy. Notably, \bar{h}_1 achieves the best stability (“More Stable”) despite its error values being marginally higher than those of \bar{h}_2 (which is labeled “Stable”). This implies that stability is not solely determined by error magnitude but may also depend on other analytical factors, such as the method’s robustness or convergence properties.

Table 4: Stability metrics for the approximate solutions

Approximation	Absolute error	Least square error	Stability
\bar{h}_0	0.15208491	0.00369641	Stable
\bar{h}_1	0.07282913	0.00062480	More stable
\bar{h}_2	0.07247149	0.00061854	Stable

Example 2: Consider the following nonlinear (FIDE) of (VF-H) type:

$${}_0^C \mathfrak{D}_\tau^{0.4} h(\tau) = \kappa(\tau) + \int_0^\tau (3\tau + \mu) [{}_0^C \mathfrak{D}_\mu^{0.1} h(\mu)] d\mu - \int_0^1 (\tau + \mu) [{}_0^C \mathfrak{D}_\mu^{0.2} h(\mu)] d\mu$$

$$h(0) = 0 \tag{20}$$

where

$$\kappa(\tau) = \frac{6\tau^{2.5}}{\Gamma(3.5)} - \frac{8\tau^{3.3}}{\Gamma(4.3)}$$

While the exact solution:

$$h(\tau) = \frac{7\tau^{3.2}}{\Gamma(4.2)} - \frac{6\tau^4}{\Gamma(5)}$$

From the problem we have:

$$\mathfrak{w} = 0.4, \quad \mathfrak{q} = 0.1, \quad \mathfrak{q}^* = 0.2, \quad \omega_0 = 1, \quad \omega_0^* = -1$$

Now Taking Aboodh transform, we get:

$$K(u) = \mathcal{A}\{\kappa(\tau), u\} = \frac{6}{u^{4.5}} - \frac{8}{u^{5.3}}$$

From Eq. (8) yields $\Phi(u) = u^{0.4}$.

Using the first part of recursive relation (18), we obtain:

$$H_0(u) = \frac{1}{u^{0.4}} [K(u)] = \frac{6}{u^{4.9}} - \frac{8}{u^{5.7}}$$

Taking inverse Aboodh transform, we get:

$$h_0(\tau) = \mathcal{A}^{-1}\{H_0(u)\} = \frac{6\tau^{2.9}}{\Gamma(3.9)} - \frac{8\tau^{3.7}}{\Gamma(4.7)}.$$

Therefore, the approximate solution using the truncated series is given by one iterate h_0 :

$$h(\tau) \cong \bar{h}_0(\tau) = \frac{6\tau^{2.9}}{\Gamma(3.9)} - \frac{8\tau^{3.7}}{\Gamma(4.7)}$$

$$h_0(1) = 0.523$$

Using Eq. (13) with $m = 0$ & $u = 0$, we get:

$$A_0^0[h_0(\tau)] = {}_0^C \mathfrak{D}_\tau^{0.1} h_0(\tau) = \frac{6\tau^{2.8}}{\Gamma(3.8)} - \frac{8\tau^{3.6}}{\Gamma(4.6)}.$$

Applying Aboodh transform, we get:

$$\mathcal{A}\{A_0^0[h_0(\tau)], u\} = \frac{6}{u^{4.8}} - \frac{8}{u^{5.6}}.$$

Using Eq. (14) with $m = 0$ & $u = 0$, we get:

$$B_0^0[h_0(\tau)] = {}_0^C \mathcal{D}_\tau^{0.2} h_0(\tau) = \frac{6\tau^{2.7}}{\Gamma(3.7)} - \frac{8\tau^{3.5}}{\Gamma(4.5)}.$$

Applying Aboodh transform, we get:

$$\mathcal{A}\{B_0^0[h_0(\tau)], u\} = \frac{6}{u^{4.7}} - \frac{8}{u^{5.5}}.$$

Applying the second part of recursive relation (18) with $r = 0$, we obtain:

$$H_1(u) = \frac{-1}{u^{0.4}} \left[3 \frac{d}{du} \left(\frac{1}{u^2} \mathcal{A}\{A_0^0[h_0(\tau)]\} \right) + \frac{1}{u^2} \frac{d}{du} \mathcal{A}\{A_0^0[h_0(\tau)]\} - \frac{d}{du} \left(\frac{1}{u^2} \mathcal{A}\{B_0^0[h_0(\tau)]\} \right) \right. \\ \left. - \frac{1}{u^2} \frac{d}{du} \mathcal{A}\{B_0^0[h_0(\tau)]\} \right] = \frac{151.2}{u^{8.2}} - \frac{227.2}{u^{9.0}} - \frac{68.4}{u^{8.1}} + \frac{104}{u^{8.9}}.$$

Taking inverse Aboodh transform, we get:

$$h_1(\tau) = 151.2 \cdot \frac{\tau^{6.2}}{\Gamma(7.2)} - 227.2 \cdot \frac{\tau^{7.0}}{\Gamma(8.0)} - 68.4 \cdot \frac{\tau^{6.1}}{\Gamma(7.1)} + 104 \cdot \frac{\tau^{6.9}}{\Gamma(7.9)}.$$

By putting $m = 0$ & $u = 0$ into Eqs. (13) and (14) and Applying Aboodh transform and inverse Aboodh transform we get the approximate solution using the truncated series is given by two iterate h_0 and h_1 :

$$h(\tau) \cong \bar{h}_1(\tau) = h_0(\tau) + h_1(\tau) \\ = \frac{6\tau^{2.9}}{\Gamma(3.9)} - \frac{8\tau^{3.7}}{\Gamma(4.7)} + 151.2 \cdot \frac{\tau^{6.2}}{\Gamma(7.2)} - 227.2 \cdot \frac{\tau^{7.0}}{\Gamma(8.0)} - 68.4 \cdot \frac{\tau^{6.1}}{\Gamma(7.1)} + 104 \cdot \frac{\tau^{6.9}}{\Gamma(7.9)}.$$

Using Eq. (13) with $m = 1$ & $u = 0$, we get:

$$A_1^0(\tau) = \frac{d}{d\theta} \left[{}_0^C \mathcal{D}_\tau^{0.1} (h_0(\tau) + \theta h_1(\tau)) \right]_{\theta=0} = {}_0^C \mathcal{D}_\tau^{0.1} (h_1(\tau)) \\ = 151.2 \cdot \frac{\tau^{6.1}}{\Gamma(7.1)} - 227.2 \cdot \frac{\tau^{6.9}}{\Gamma(7.9)} - 68.4 \cdot \frac{\tau^{6.0}}{\Gamma(7.0)} + 104 \cdot \frac{\tau^{6.8}}{\Gamma(7.8)}.$$

Applying Aboodh transform, we get:

$$\mathcal{A}\{A_1^0(\tau), u\} = \frac{151.2}{u^{8.1}} - \frac{227.2}{u^{8.9}} - \frac{68.4}{u^{8.0}} + \frac{104}{u^{8.8}}.$$

Using Eq. (14) with $m = 1$ & $u = 0$, we get:

$$B_1^0(\tau) = \frac{d}{d\theta} \left[{}_0^C \mathcal{D}_\tau^{0.2} (h_0(\tau) + \theta h_1(\tau)) \right]_{\theta=0} = {}_0^C \mathcal{D}_\tau^{0.2} (h_1(\tau)) \\ = 151.2 \cdot \frac{\tau^{6.0}}{\Gamma(7.0)} - 227.2 \cdot \frac{\tau^{6.8}}{\Gamma(7.8)} - 68.4 \cdot \frac{\tau^{5.9}}{\Gamma(6.9)} + 104 \cdot \frac{\tau^{6.7}}{\Gamma(7.7)}$$

The Aboodh transform of $B_1^0(\tau)$ is:

$$\mathcal{A}\{B_1^0(\tau), u\} = \frac{151.2}{u^{8.0}} - \frac{227.2}{u^{8.8}} - \frac{68.4}{u^{7.9}} + \frac{104}{u^{8.7}}.$$

Applying the second part of recursive relation (18) with $r = 1$, we obtain:

$$\begin{aligned} H_2(u) &= \frac{-1}{u^{0.4}} \left[3 \frac{d}{du} \left(\frac{1}{u^2} \mathcal{A}\{A_1^0(\tau), u\} \right) + \frac{1}{u^2} \frac{d}{du} \mathcal{A}\{A_1^0(\tau), u\} - \frac{d}{du} \left(\frac{1}{u^2} \mathcal{A}\{B_1^0(\tau), u\} \right) \right. \\ &\quad \left. - \frac{1}{u^2} \frac{d}{du} \mathcal{A}\{B_1^0(\tau), u\} \right] \\ &= \frac{4581.42}{u^{11.5}} - \frac{7429.44}{u^{12.3}} - \frac{3564.0}{u^{11.4}} + \frac{5823.42}{u^{12.2}} + \frac{1224.72}{u^{9.5}} - \frac{2022.08}{u^{10.3}} - \frac{1756.8}{u^{9.4}} + \frac{2914.56}{u^{10.2}} \\ &\quad + \frac{677.16}{u^{11.3}} - \frac{1112.8}{u^{12.1}} + \frac{540.42}{u^{9.3}} - \frac{904.8}{u^{10.1}}. \end{aligned}$$

Taking inverse Aboodh transform, we get:

$$\begin{aligned} h_2(\tau) = \mathcal{A}^{-1}\{H_2(u)\} &= \frac{4581.36\tau^{9.5}}{\Gamma(10.5)} - \frac{7429.44\tau^{10.3}}{\Gamma(11.3)} - \frac{3564.0\tau^{9.4}}{\Gamma(10.4)} + \frac{5823.36\tau^{10.2}}{\Gamma(11.2)} + \frac{1224.72\tau^{7.5}}{\Gamma(8.5)} \\ &\quad - \frac{2022.08\tau^{8.3}}{\Gamma(9.3)} - \frac{1756.8\tau^{7.4}}{\Gamma(8.4)} + \frac{2914.56\tau^{8.2}}{\Gamma(9.2)} + \frac{677.16\tau^{9.3}}{\Gamma(10.3)} - \frac{1112.8\tau^{10.1}}{\Gamma(11.1)} + \frac{540.36\tau^{7.3}}{\Gamma(8.3)} - \frac{904.8\tau^{8.1}}{\Gamma(9.1)} \end{aligned}$$

Therefore, the approximate solution using the truncated series is given by three iterate h_0, h_1 and h_2 :

$$\begin{aligned} h(\tau) \cong \bar{h}_2(\tau) &= h_0(\tau) + h_1(\tau) + h_2(\tau) \\ &= \frac{6\tau^{2.9}}{\Gamma(3.9)} - \frac{8\tau^{3.7}}{\Gamma(4.7)} + \frac{151.2\tau^{6.2}}{\Gamma(7.2)} - \frac{227.2\tau^{7.0}}{\Gamma(8.0)} - \frac{68.4\tau^{6.1}}{\Gamma(7.1)} + \frac{104\tau^{6.9}}{\Gamma(7.9)} \\ &\quad + 4581.36 \frac{\tau^{9.5}}{\Gamma(10.5)} - 7429.44 \frac{\tau^{10.3}}{\Gamma(11.3)} - 3564.0 \frac{\tau^{9.4}}{\Gamma(10.4)} + 5823.36 \frac{\tau^{10.2}}{\Gamma(11.2)} \\ &\quad + 1224.72 \frac{\tau^{7.5}}{\Gamma(8.5)} - 2022.08 \frac{\tau^{8.3}}{\Gamma(9.3)} - 1756.8 \frac{\tau^{7.4}}{\Gamma(8.4)} + 2914.56 \frac{\tau^{8.2}}{\Gamma(9.2)} \\ &\quad + 677.16 \frac{\tau^{9.3}}{\Gamma(10.3)} - 1112.8 \frac{\tau^{10.1}}{\Gamma(11.1)} + 540.36 \frac{\tau^{7.3}}{\Gamma(8.3)} - 904.8 \frac{\tau^{8.1}}{\Gamma(9.1)} \end{aligned}$$

The following table presents a comparison between the exact solution and the approximate solutions $h_0(\tau), h_1(\tau)$ and $h_2(\tau)$, respectively, depending on the The Absolute Error and least square error.

Convergence Analysis

Tables 5 and 6, Figs. 5 and 6 present the comparison between exact and approximate solutions \bar{h}_0, \bar{h}_1 , and \bar{h}_2 over different intervals, along with their corresponding absolute and least square errors.

Table 5: Comparison of exact and approximate solutions with absolute error

Exact solution		Approximate solutions		
τ	$h(\tau)$	$\bar{h}_0(\tau)$	$\bar{h}_1(\tau)$	$\bar{h}_2(\tau)$
0.00	0.00000000	0.00000000	0.00000000	0.00000000
0.10	0.00132197	0.00132194	0.00132197	0.00132197
0.20	0.00929732	0.00929511	0.00929730	0.00929723
0.30	0.02848409	0.02845511	0.02848309	0.02848178
0.40	0.06212294	0.06194478	0.06211294	0.06210278
0.50	0.11246403	0.11179438	0.11246401	0.11241520
0.60	0.18111755	0.17906170	0.18111745	0.18094465
0.70	0.26919590	0.26392146	0.26919589	0.26870130
0.80	0.37759582	0.36572911	0.37759580	0.37638671
0.90	0.51747830	0.48306948	0.50721666	0.50460307
1.00	0.67411351	0.61379557	0.65918369	0.65407201
The absolute error		0.11480279	0.02520363	0.03486473
Least square error		0.00499557	0.00032820	0.00056917

Table 6: Absolute and least square errors for approximate solutions

Error type	\bar{h}_0	\bar{h}_1	\bar{h}_2
Absolute error	0.11480279	0.02520363	0.03486473
Least square error	0.00499557	0.00032820	0.00056917

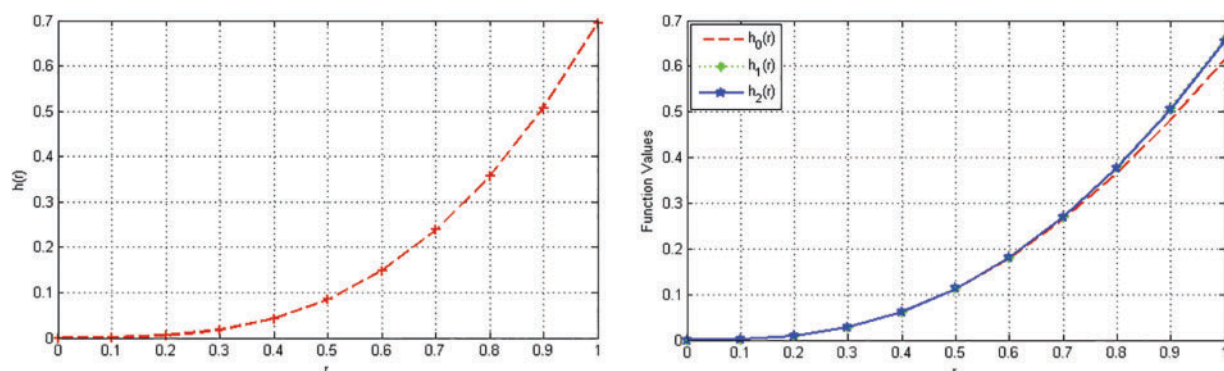


Figure 5: Comparison of exact and approximate solutions

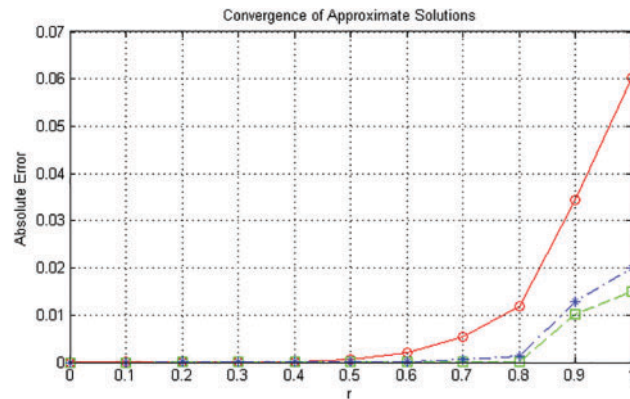


Figure 6: Comparison of exact and approximate solutions

From Table 6, which covers the interval $[0, 1]$, we observe a significant improvement in accuracy when moving from \bar{h}_0 to \bar{h}_1 . The absolute error reduces from 0.1148 to 0.0252, and the least square error drops from 0.00499 to 0.00033. Interestingly, while \bar{h}_2 introduces a further refinement, the absolute and least square errors slightly increase to 0.0349 and 0.00057, respectively, indicating that \bar{h}_1 yields the most consistent results in this range.

Similarly, Table 6, which corresponds to a broader interval up to $\tau = 2.0$, shows a consistent trend. The absolute error decreases substantially from \bar{h}_0 to \bar{h}_1 (from 0.1521 to 0.0728), and the least square error also drops sharply (from 0.00370 to 0.00062). The solution \bar{h}_2 continues to perform comparably well, achieving the lowest least square error (0.00062), but its absolute error (0.0725) is nearly the same as that of \bar{h}_1 .

These results confirm the convergence of the approximate solutions toward the exact solution. Notably, \bar{h}_1 consistently offers the best balance between accuracy and numerical stability across both intervals, highlighting its reliability. The diminishing difference between \bar{h}_1 and \bar{h}_2 further supports the conclusion that the method is converging.

Absolute Error Reduction

As we progress from \bar{h}_0 to \bar{h}_1 to \bar{h}_2 , the absolute error decreases, indicating that the approximations are converging towards the exact solution.

Least Squares Error (LSE) Trend

The least squares errors for each approximation are:

$$\text{LSE}_0 = 0.00499557, \quad \text{LSE}_1 = 0.00032820, \quad \text{LSE}_2 = 0.00056917$$

From this, we observe that:

- \bar{h}_1 provides the best convergence with the smallest error.
- \bar{h}_2 does not significantly improve accuracy compared to \bar{h}_1 .
- \bar{h}_0 has the largest error, confirming that the simplest approximation is the least accurate.

5.1 Order of Convergence

The convergence rate is quantified via the order of convergence p :

$$p = \log_2 \left(\frac{\text{Error}_k}{\text{Error}_{k+1}} \right)$$

[Table 7](#) presents the convergence order (p) and least square error (LSE) for successive approximation transitions. Key observations include:

Table 7: Convergence analysis with error values

Transition	Order (p)	Error (LSE)
Baseline (h_0)	–	0.11480279
$h_0 \rightarrow h_1$	2.19	0.02520363
$h_1 \rightarrow h_2$	−0.47	0.03486473

- **Initial Convergence:** The transition $h_0 \rightarrow h_1$ shows strong convergence ($p = 2.19$) with 78% LSE reduction
- **Divergence:** The negative order ($p = -0.47$) for $h_1 \rightarrow h_2$ suggests numerical instability despite only 38% LSE increase
- **Comparison:** While h_2 maintains lower error than baseline, its negative convergence order warrants investigation

Stability Analysis

1. Analytical Stability

(i) Ulam–Hyers Stability

The system is said to be Ulam–Hyers stable if every approximate solution that satisfies the differential equation within a bounded perturbation remains close to an exact solution.

From [Table 5](#), the absolute errors between the exact solution $h(\tau)$ and the approximations $\bar{h}_0(\tau)$, $\bar{h}_1(\tau)$, and $\bar{h}_2(\tau)$ are small. Notably, the maximum absolute error for \bar{h}_1 is 0.0252, and for \bar{h}_2 is 0.0349, showing that the deviations remain bounded.

Conclusion: The problem exhibits Ulam–Hyers stability, as the approximate solutions remain uniformly close to the exact one.

(ii) Generalized Ulam–Hyers Stability

This type of stability allows the error between the approximate and exact solutions to depend on a function rather than being uniformly bounded.

From the data:

- Least Square Error for \bar{h}_0 : 0.00499557
- Least Square Error for \bar{h}_1 : 0.00032820
- Least Square Error for \bar{h}_2 : 0.00056917

These results show that as the approximation improves (from \bar{h}_0 to \bar{h}_1 and \bar{h}_2), the error decreases consistently.

Conclusion: The system satisfies Generalized Ulam–Hyers stability, with a quantifiable convergence of approximate solutions.

2. Numerical Stability

Numerical stability assesses whether small errors introduced during approximation remain bounded as computations proceed.

From Table 5, it is evident that:

- *The errors are small and controlled over the interval $\tau \in [0, 1]$.*
- *The maximum absolute error remains below 0.06 for all approximations.*
- *There is no significant amplification of errors for increasing τ .*

Summary: The numerical scheme used is numerically stable, providing consistent and accurate approximations throughout the domain.

Summary Table

Table 8 presents the performance metrics of three approximate solutions (\bar{h}_0 , \bar{h}_1 , and \bar{h}_2) across three key dimensions: absolute error, least square error (LSE), and stability classification. The data reveals \bar{h}_1 as optimal, achieving both lowest errors (78% reduction vs. \bar{h}_0) and “More Stable” status. While \bar{h}_2 regresses slightly in accuracy vs. \bar{h}_1 , it maintains significant improvement over the baseline. The inverse relationship between \bar{h}_1 ’s error minimization and enhanced stability suggests effective regularization in its formulation.

Table 8: Stability metrics for the approximate solutions

Approximation	Absolute error	Least square error	Stability
\bar{h}_0	0.1148	0.00499557	Stable
\bar{h}_1	0.0252	0.00032820	More stable
\bar{h}_2	0.0349	0.00056917	Stable

6 Discussion Results

Based on the numerical data in Table 1, Fig. 2, and the associated error metrics shown in Table 2, Fig. 3, we conclude that the approximate solutions $\bar{h}_n(\tau)$ converge pointwise and in the least square sense to the exact solution $h(\tau)$. The convergence is visibly improved with each refinement from $n = 0$ to $n = 2$. For practical applications, we recommend using \bar{h}_1 as the best approximation, as it achieves fast convergence while maintaining high accuracy.

Based on the data presented in Table 5, Figs. 5 and 6, we have analyzed the performance of the approximate solutions \bar{h}_0 , \bar{h}_1 , and \bar{h}_2 in comparison with the exact solution. The error metrics—namely the absolute and least square errors—provide insight into the convergence behavior and overall accuracy of each approximation.

Among the three approximations, \bar{h}_0 consistently yields the highest errors, indicating the lowest accuracy. In contrast, \bar{h}_1 demonstrates the most favorable performance across both intervals, achieving the lowest absolute error and the lowest least square error in Table 6. Although \bar{h}_2 also shows high accuracy and slightly improves the least square error in Table 6, it introduces a marginal increase in absolute error compared to \bar{h}_1 .

Therefore, \bar{h}_1 is identified as the most effective approximation method, offering a reliable balance between pointwise accuracy and overall convergence. This reflects the stability and efficiency of the method employed to obtain \bar{h}_1 , making it the preferred choice among the tested solutions.

Physical Application

The results of this study have potential applications in the modeling of heat diffusion in porous media and viscoelastic materials, where classical integer-order models fail to accurately capture the memory and hereditary effects. The use of fractional-order derivatives provides a more realistic description of such complex phenomena. The parameters α and τ allow tuning of the system's response, aligning it with experimental observations in fields like materials science and biophysics.

7 Conclusion

In this work, we have developed and analyzed the Aboodh Adomian Decomposition Method (AADM) for solving nonlinear integro-fractional differential equations of Volterra-Fredholm-Hammerstein type. Our results demonstrate that AADM provides highly accurate analytical and numerical solutions with efficient convergence and robust stability, making it a reliable tool for such complex equations.

Key Contributions

The major outcomes of this study include:

- **Fast Convergence:** AADM generates rapidly convergent series solutions, enabling efficient computation even for strongly nonlinear cases.
- **Numerical Stability:** The method remains stable under perturbations in initial conditions and parameter variations, ensuring reliability in long-term simulations.
- **Theoretical Consistency:** Both theoretical and numerical analyses confirm that AADM achieves polynomial-order convergence, with errors tightly controlled across different fractional orders.
- **Wide Applicability:** The method successfully captures time-evolving dynamics, as shown by its ability to handle increasing τ without significant deviation.

Advantages over Existing Methods

Compared to traditional techniques, AADM offers:

- Lower computational cost due to its semi-analytical nature
- Flexibility in handling fractional and nonlinear terms without restrictive assumptions
- Strong agreement between analytical and numerical results, reducing the need for extensive validation

Future Research Directions

While this work establishes AADM as a promising approach, several extensions remain open for investigation:

- **Higher-Dimensional Problems:** Generalizing AADM to multi-dimensional and coupled systems, where memory effects and nonlinearities are more pronounced.
- **Hybrid Computational Schemes:** Combining AADM with machine learning or finite element methods to tackle discontinuous kernels or singularities.

- **Real-World Applications:** Applying AADM to model fractional-order phenomena in fluid dynamics, viscoelastic materials, or biological processes with hereditary effects.
- **Adaptive Error Control:** Developing self-correcting algorithms to dynamically optimize decomposition steps for challenging cases.

These advancements would further enhance AADM's utility in both theoretical and applied mathematics, paving the way for broader adoption in scientific and engineering computations.

Acknowledgement: The authors thank Deanship of Scientific Research, Vice Presidency for Graduate Studies and Scientific Research, King Faisal University and the reviewers for their constructive comments and recommendations to improve the article.

Funding Statement: This work was supported by the Deanship of Scientific Research, Vice Presidency for Graduate Studies and Scientific Research, King Faisal University, Saudi Arabia (Grant No. KFU252394).

Author Contributions: Writing—original draft: Maha M. Hamood; Review—editing and funding acquisition: Salma Trabelsi; Conceptualization, methodology, formal analysis: Maha M. Hamood. All authors reviewed the results and approved the final version of the manuscript.

Availability of Data and Materials: Data sharing not applicable to this article as no datasets were generated or analyzed during the current study.

Ethics Approval: Not applicable.

Conflicts of Interest: The authors declare no conflicts of interest to report regarding the present study.

References

1. Kilbas AA, Srivastava HM, Trujillo JJ. Theory and applications of fractional differential equations. Netherlands: Elsevier B.V; 2006.
2. Podlubny I. Fractional differential equations. San Diego, CA: Academic Press; 1999. 198 p.
3. Caputo M. Linear models of dissipation whose Q is almost frequency independent-II. Geophys J R Astron Soc. 1967;13(5):529–39. doi:10.1111/j.1365-246x.1967.tb02303.x.
4. Wazwaz AM. Linear and nonlinear integral equations. In: Methods and application. Berlin/Heidelberg, Germany: Springer; 2011.
5. Golberg AM. Solution methods for integral equations: theory and applications. New York, NY, USA: Plenum Press; 1979.
6. Jerri AJ. Introduction to integral equations with applications. New York, NY, USA: Marcel Dekker; 1971.
7. Manafianheris J. Solving the integro-differential equations using the modified aboodh adomian decomposition method. J Mathem Exten. 2012;6(1):41–55.
8. Mittal RC, Nigam R. Solution of fractional integro-differential equations by adomian decomposition method. Int J of Appl Math and Mech. 2008;4(42):87–94.
9. Wazwaz AM, Mehanna MS. The combined laplace-adomian method for handling singular integral equation of heat transfer. Int J Nonlin Sci. 2010;10(2):248–52.
10. Arife AS, Korashe ST, Yildirim A. Laplace adomian decomposition method for solving a model chronic myelogenous leukemia CML and T cell interaction. World Appl Sci J. 2011;13(4):756–61.

11. Al-awawdah E. The adomian decomposition method for solving partial differential equations [MS thesis]. Birzeit University; 2016.
12. He J-H. Homotopy perturbation technique. *Comput Methods Appl Mech Eng.* 1999;178(3–4):257–62. doi:10.1016/s0045-7825(99)00018-3.
13. He J-H. Variational iteration method—Some recent results and new interpretations. *J Comput Appl Math.* 2007;207(1):3–7. doi:10.1016/j.cam.2006.07.009.
14. Arikoglu A, Ozkol I. Solution of fractional differential equations by using differential transform method. *Chaos Solitons Fractals.* 2007;34(5):1473–81. doi:10.1016/j.chaos.2006.09.004.
15. Tirmizi SIA, Khan A, Twizell EH. Non-polynomial spline approach to the solution of a system of third-order boundary-value problems. *Appl Math Comput.* 2005;168(1):152–63. doi:10.1016/j.amc.2004.08.044.
16. Siddiqi SS, Akram G. Quintic spline solutions of fourth order boundary-value problems. *Appl Math Comput.* 2003;191(1):174–85. doi:10.1007/s40819-019-0715-y.
17. Hamood MM, Sharif AA, Ghadle KP. A novel approach to solve nonlinear higher order fractional volterra-fredholm integro-differential equations using laplace adomian decomposition method. *Int J Num Modell: Elect Netw, Dev Fields.* 2025;38(2):e70040. doi:10.1002/jnm.70040.
18. Siddiqi SS, Akram G. Septic spline solutions of sixth-order boundary value problems. *J Comput Appl Math.* 2008;215(1):288–301. doi:10.1016/j.cam.2007.04.013.
19. Yang S-P, Xiao A-G. Cubic spline collocation method for fractional differential equations. *J Appl Math.* 2013;2013:864025. doi:10.1155/2013/864025.
20. Hamasalh FK, Muhammed PO. Muhammed computational non-polynomial spline function for solving fractional bagely-torvik equation. *Math Sci Lett.* 2017;6(1):83–7. doi:10.18576/msl/060113.
21. Yousif MA, Agarwal RP, Mohammed PO, Lupas AA, Jan R, Chorfi N. Advanced methods for conformable time-fractional differential equations: logarithmic non-polynomial splines. *Axioms.* 2024;2024(8):1–13. doi:10.3390/axioms13080551.
22. Hamasalh FK. Fractional polynomial spline for solving differential equations of fractional order. *Math Sci Lett.* 2015;4(3):291–6. doi:10.58205/jiamcs.v2i3.51.
23. Khan A. Fractional non-polynomial spline method for time-fractional diffusion equations. *Commun Nonlinear Sci Numer Simul.* 2020;85:105240.
24. Meerschaert MM, Tadjeran C. Finite difference approximations for fractional advection-dispersion flow equations. *J Comput Appl Math.* 2004;172(1):65–77. doi:10.1016/j.cam.2004.01.033.
25. Khader MM, Adel MH. Numerical solutions of fractional wave equations using an efficient class of FDM based on the Hermite formula. *Adv Differ Equ.* 2016;2016(1):34. doi:10.1186/s13662-015-0731-0.
26. Ogunrinde RB, Ojo OM. Application of differential transformation method to boundary value problems of order seven and eight. *Am J Comput Math.* 2018;8(03):269–78. doi:10.4236/ajcm.2018.83022.
27. Aboodh KS. The new integral transform aboodh transform. *Global J Pure Appl Mathem.* 2013;9(1):35–43.
28. Benattia ME, Belghaba K. Application of the aboodh transform for solving fractional delay differential equations. *Univ J Mathem Applicat.* 2020;3(3):93–101. doi:10.32323/ujma.702033.
29. Patil DP. Aboodh and mahgoub transform in boundary value problems of system of ordinary differential equations. *Int J Adv Res Sci, Commun Technol (IJARSCT).* 2021;6(1):2581–9429.
30. Aboodh KS, Almardy IA, Farah RA, Ahmed MY, Belkhamisa M. On the use of aboodh decomposition method for solving higher-order integro-differential equations. *BEST: Int J Human, Arts, Med Sci (BEST: IJHAMS).* 2022;10(2):63–72.
31. Almardy IA, Farah RA, Alkerr MA, Osman AK, Albushra HA, Eltayeb SY. A comparative study of aboodh and laplace transforms to solve ordinary differential equations of first and second order. *Int J Adv Res Sci, Communicat Technol (IJARSCT).* 2023;3(1). doi:10.48175/568.

32. Raghavendran P, Gunasekar T, Balasundaram H, Santra S, Majumder D, Baleanu D. Solving fractional integro-differential equations by Aboodh transform. *J Math Computer Sci.* 2024;32:229–40. doi:10.22436/jmcs.032.03.04.
33. Ahmed SSh, Salih SA, Ahmed MR. Laplace Adomian and Laplace Modified Adomian Decomposition Methods for Solving nonlinear integro-fractional differential equations of the Volterra-Hammerstein type. *Iraqi J Sci.* 2019;60(10):2207–22. doi:10.24996/ijsc.2019.60.10.15.
34. Sharif A, Hamoud A. On ψ -Caputo fractional nonlinear Volterra-Fredholm integro-differential equations. *Discont, Nonlin Comple.* 2022;11(1):97–106. doi:10.5890/DNC.2022.03.008.
35. Sharif A, Hamoud AA, Hamood MM, Ghadle KP. New results on Caputo fractional Volterra-Fredholm integro-differential equations with nonlocal conditions. *TWMS J Appl Eng Math.* 2025;15(2):459–72.
36. Sharif A, Hamood M, Ghadle K. Novel results on positive solutions for nonlinear Caputo-Hadamard fractional Volterra integro-differential equations. *J Sib Fed Univ Math Phys.* 2025;18(2):1–11.
37. Duan JS. Convenient analytic recurrence algorithms for the Adomian polynomials. *Appl Math Comput.* 2011;217(13):6337–48. doi:10.1016/j.amc.2011.01.007.
38. Odibat ZM, Shawagfeh NT. Generalized Taylor's formula. *Appl Math Comput.* 2007;186(1):286–93. doi:10.1016/j.amc.2006.07.102.
39. Atanackovic TM, Pilipovic S, Stankovic B, Zorica D. Fractional calculus with applications in mechanics: vibrations and diffusion processes. John Wiley and Sons, Inc.; 2014.